2.   ACCELERATOR AUGMENTATION PROGRAM

2.1   LINAC

S.Ghosh,   R.Mehta,   G.K.Chowdhury,   A.Rai,   P.Patra,   B.K.Sahu, A.Pandey,   D.S.Mathuria, S.S.K.Sonti, K.K.Mistry, R.N. Dutt, J.Chacko, A.Chowdhury, S. Kar, S.Babu, M.Kumar, R.S.Meena, J. Zacharias, P.N.Prakash, T.S.Datta, A.   Mandal, D.Kanjilal and A.Roy

2.1.1   Activities related to Superconducting Linear Accelerator

The commissioning of the superconducting booster linac, to boost the energy of ion beams from the existing 15 UD Pelletron, has reached the final stage. At present, the superbuncher (SB) cryostat housing a single niobium quarter wave resonator (QWR), the first accelerating module containing eight QWRs and the rebuncher (RB) cryostat housing two QWRs are operational. The remaining two accelerating modules including the cryostats and sixteen QWRs are in the final stage of fabrication and will be installed and commissioned by the end of 2009. Ion beams from Pelletron accelerator were accelerated and delivered for conducting experiments in the past with the help of SB, the first linac module and the RB [1]. However, the problem of helium leak from the SS-welded bellows attached in the coupling and beam ports of the resonator cropped up intermittently. This posed a serious threat to the reliable and consistent operation of linac. It was thus decided, that all the coupling and beam port flanges with SS edge welded bellows would be replaced by flanges with SS formed bellows irrespective of whether they were leaking or not. The details of the leak problems and their solution are presented in the following subsections.

The frequency control of the superconducting quarter wave resonator is currently accomplished by mechanical and electronic tuners which are operated in the time scale of a few seconds to a few microseconds. During operation, input RF power ≤ 100 W was required to control the resonator for a typical field of 3-5 MV/m for 6 watts of power dissipated in liquid helium. Though resonators are working fine at this power level, investigations are going on whether more reliable operation of the resonators is possible using a piezoelectric actuator to control the amplitude and phase of the accelerating fields. The preliminary test results of the Piezo electric actuator are mentioned in the last subsection.

2.1.1.1 The solution of the helium leaks from the coupling/beam port flanges of Niobium resonator

The cross-sectional view and the photograph of the resonator are shown in figure 2 (a) and (b) respectively. The resonator is formed of bulk niobium and is jacketed by another enclosure made of stainless steel. Liquid helium (LHe) is poured into the central conductor as

well as inside the annular space between the two concentric cylinders to make it bath cooled. A transition flange made by explosively bonded niobium-SS material is used to provide the welding transition between niobium and SS places where the outer stainless steel jacket joins the niobium resonator (to provide power coupling ports, pick-up ports and open end flanges at the tuner end). Details of the design have been presented elsewhere [2, 3].

(a)   **(b)**
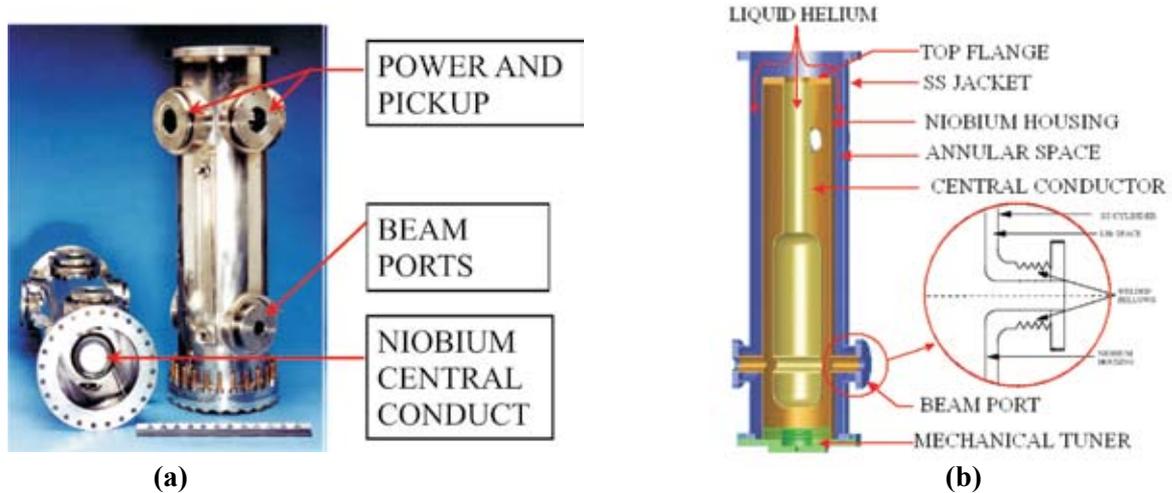
**Fig.1. (a) The cross-sectional view and (b) the photograph of the resonator
with beam/coupling ports and SS-jacket**

Since the liquid helium enclosure was made of SS, explosively bonded Nb-SS transition flanges were used to join the coupling/beam ports and the open end flange at the tuner side of the resonator. Edge welded SS bellows were used in all the coupling/beam ports of the first twelve resonators (shown in figure 2) to accommodate the differential contraction between niobium and SS at 4.2 K.

**Fig.2. Transition flanges with SS-Edge welded bellows (shown in left) are now replaced with
the transition flanges with SS-formed bellows (shown in right)**

16

After a few thermal cycles, the thin edge welded SS-bellows started leaking in pressurized condition causing deterioration of the cryostat vacuum. The thin edge welded bellows of eleven QWRs were subsequently replaced by thicker formed SS-bellows (shown in figure 2) and with this modification, the leaks from the bellows have been eliminated.

2.1.1.2 Successful test of the Piezoelectric crystal as frequency tuner of SC QWR

The vibration induced frequency fluctuations (~ a few tens of Hz) in the bulk niobium resonators of IUAC, have got slow (in time scale of seconds) and fast (few tens to hundreds of μsec) components. To arrest the fast drifts of frequency, the effective bandwidth is increased by over-coupling the resonator with respect to the RF amplifier. The slow drift of the frequency is controlled by flexing the niobium bellows acting as the mechanical tuner. The two tuning mechanisms working simultaneously are able to lock the phase and amplitude of the resonators with respect to master oscillator. However, mechanical tuning using high purity helium gas is complicated and expensive. The recent growing usage of piezoelectric crystals in the tuning mechanism of SC resonators has made the tuning mechanism more reliable and cost effective. A study and development of a piezoelectric tuning mechanism with our existing fast tuning control scheme based on Dynamic Phase Control method for the phase locking of the resonator was undertaken.
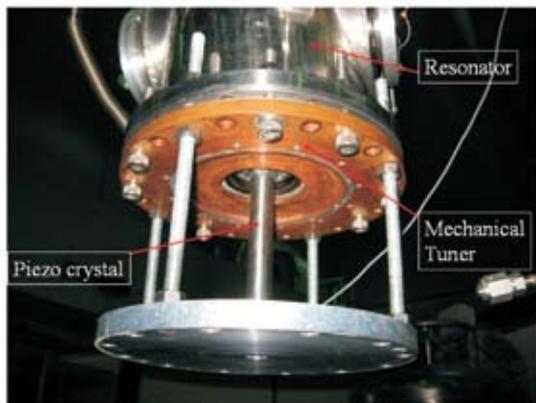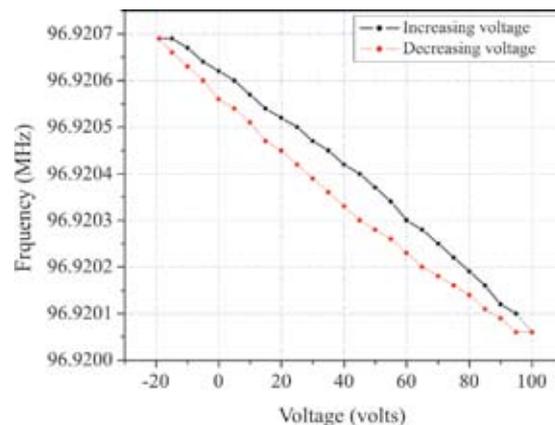
(a)   (b)

Fig.3. (a) The Piezo crystal is connected with the mechanical tuner prior to loading in test cryostat, (b) Hysteresis curve of the Piezo actuator

The Piezo crystal (Physik Instrumente (PI) make) was connected to the bottom (figure 3(a)) of the niobium mechanical tuner of the resonator. It was powered by a supply in the range of -19 to 100 V to measure its total tuning range. The frequency variation with the Piezo tuner attached with a QWR was measured to be ~2.5 kHz and ~626 Hz at room temperature and at 4.2 K respectively. The hysteresis observed in the frequency change for increase and decrease of the bias voltage of the piezoelectric actuator in cold condition is shown in figure 3(b).

A PI based control scheme was built to compensate the frequency drift around the central frequency of the resonator and to eliminate the hysteresis effects by generating an appropriate voltage for the piezoelectric tuner according to the phase error of the resonator controller. During the first test of a superconducting resonator in test cryostat along with the fast tuner and piezoelectric actuator acting as slow tuner, the overall locking mechanism worked very well. The stability of the lock was observed for an hour at a moderate accelerating field of 2.2 MV/m. The amplitude and phase lock stabilities were measured to be 0.1% and ±0.4 degree respectively at this field level. The resonator was also locked at 3.0 MV/m for a short duration, but due to lack of time, stability test at this field could not be accomplished for a longer period. More detailed information about the testing of the Piezo tuner can be found out elsewhere [4].

REFERENCES

[1]   S.Ghosh, R.Mehta, G.K.Chowdhury, A.Rai, P.Patra, B.K.Sahu, A.Pandey, D.S.Mathuria, J.Chacko, A.Chowdhury, S.Kar, S.Babu, M.Kumar, S.S.K.Sonti, K.K.Mistry, J. Zacharias, P.N.Prakash, T.S.Datta, A. Mandal, D.Kanjilal and A. Roy, To be published shortly in Physical Review – Special Topic –Accelerator and Beam.

[2]   K.W. Shepard, A.Roy and P.N.Potukuchi, Proc. of the 1997 Particle Accelerator Conference, May 12-16, 1997, Vancouver, BC, Canada, page-3072.

[3]   P.N.Potukuchi, S. Ghosh and K.W. Shepard, Proc. of the 1999 Particle Accelerator Conference, New York, USA, page-952.

[4]   B.K.Sahu, S.Ghosh, R.Mehta, G.K.Chowdhury, A.Rai, P.Patra, A.Pandey, D.S.Mathuria, K. Singh, D.Kanjilal and A.Roy, Proc. of LINAC conference 2008, Sept 29 – Oct 03, 2008, British Columbia, Canada

2.1.2   Superconducting Niobium Resonators

P.N.Prakash, S.S.K.Sonti, K.K.Mistri, J.Zacharias, A.Rai, D.Kanjilal & A.Roy

The production of the niobium quarter wave resonators for the second and third linac modules is almost over. The reworking/repairing of two ANL-built resonators and one indigenously built resonator has been completed. All the three reworked resonators have been cold tested at 4.5 K and subsequently installed in the superconducting linac. Work on the construction of two Single Spoke Resonators for Project-X at Fermi National Accelerator Laboratory has been slightly delayed. However, in the last few months substantial progress was made. Under an MoU, IUAC and RRCAT, Indore have jointly started the development of a Tesla-type Single Cell Cavity in niobium.

2.1.2.1 Resonator Production for the 2nd & 3rd Linac Modules

The production of fifteen quarter wave resonators (QWRs) for the 2nd and 3rd linac modules has progressed substantially and the construction of twelve QWRs is almost over.

The bare niobium resonators have been completed and the final electropolishing (EP) and the post EP heat treatment is over. They are now ready for the outer stainless steel jacketing, which is expected to be completed in the next several weeks. The remaining three QWRs have to be slightly reworked before they can be completed. We have deliberately kept them aside to focus on completing the twelve QWRs first.

Briefly the work done during the last one year is as follows. All the resonators were tuned to the correct frequency by adjusting the central conductor length and e-beam welding them to the top flange. The assemblies were then welded to their respective housings to complete the bare niobium resonator assembly. Based on the frequency measurement on the resonators they were electropolished in two different ways. While some resonators were electropolished fully, others were first electropolished preferentially in the inductive region of the co-axial line followed by complete electropolishing of the full resonator. The number of electropolishing cycles for each resonator was decided by how far off its frequency was compared to the aimed value. However, all resonators were fully electropolished at least 50 cycles to remove 40-50 μm from the surface. This was done to ensure that a clean niobium surface was obtained before the crucial heat treatment step. All the resonators were heat treated at 1100° C in vacuum levels that were better than 5×10^{-6} mbar. Figure 1 shows some of the bare niobium resonators that have been completed.

In order to frequency tune all the resonators one Slow Tuner assembly was initially completed. All the remaining fourteen Slow Tuner assemblies are also nearing completion. The bellows assemblies have been completed and they are now ready for the final e-beam

Fig. 1. Bare niobium Quarter Wave Resonators
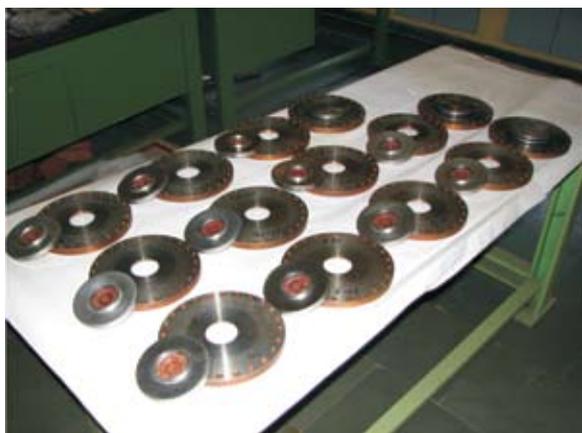
Fig. 2. Slow Tuner Bellows assemblies.

welding to the Nb-Cu flange. In order to stress relieve the bellows after cold forming and e-beam welding, but before the top disc is welded (the top disc is made from niobium explosively bonded to copper), they were annealed at 800°C in vacuum. Figure 2 shows the bellows assemblies along with the Nb-Cu flanges ready for completion. We plan to complete the final e-beam welding of all the Slow Tuners during the jacketing work on the twelve QWRs.

2.1.2.2 Reworking of QWRs

Two of the ANL-built QWRs and one indigenously built QWR had punctures on the Central Conductor at the upper cap, which is near the joint where the capacitive Drift Tube of the coaxial line joins the inductive Loading Arm. Although these resonators had been cut open during previous years they could not be worked upon since all efforts had been focused on completing the resonator production. As the resonator production reached the same stage that the repair-resonators were in, we decided to complete them along with the production resonators. The upper caps were removed from the central conductors and new caps were welded in their place. The separate assemblies were electropolished, frequency tuned, e-beam welded and heat treated. The lengths of the outer housings were adjusted to match the beam ports with their corresponding central conductors and then the closure welds were performed. This was followed by the completion of the upper portion of the stainless steel jackets.

Prior to cold testing the ANL-built QWRs were given light electropolishing to remove 5-10 μm from the surface whereas the indigenously built resonator was more heavily electropolished to remove 40-50 μm. The ANL-built resonators had been heavily electropolished before their central conductors got punctured and we did not want to risk removing further material through more electropolishing, thereby compromising with the wall thickness of the niobium material.

In cold tests at 4.5 K the performance of the indigenously built resonator QWR-I2 and one of the ANL-built resonators QWR-6 is shown in figure 3. We feel that the substantially
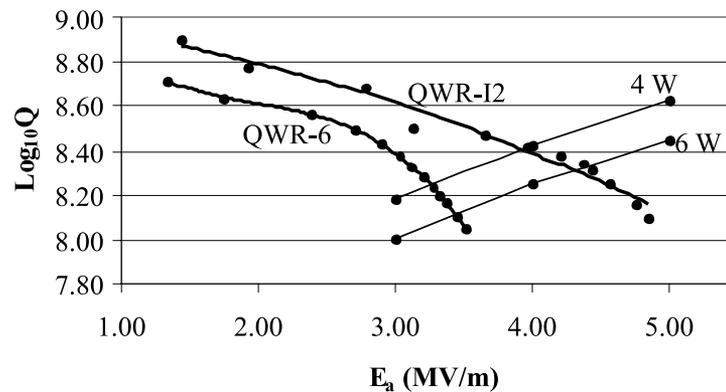
Fig. 3. Accelerating electric field Ea as a function of Q at 4.5 K.

superior performance of the indigenously built resonator is largely due to the heavy electropolishing done prior to cold testing. All the three resonators have now been installed in the linac.

2.1.2.3 Spoke Resonators

In addition to the in-house programs, IUAC is also building two Single Spoke Resonators - SSR1 (β=0.22, f=325 MHz) for Project-X at Fermi National Accelerator Laboratory (FNAL), USA. Figure 4 shows an exploded view of SSR1. The outer diameter of the resonator is approximately 500 mm. The major components of the resonator are: Shell, Spoke - which is formed in two halves and welded together, End Walls along with their Beam Ports and Donut Ribs (for stiffening), and the Spoke to Shell Collars that join the Spoke to the outer Shell.

All the components listed above are die formed except the flanges, Spoke Beam Port and the Beam Port Tubes on the End Walls. The Coupler Port & Beam Port flanges, which are made out of stainless steel, are brazed to the niobium tubes. Of all the dies required for the construction of the Spoke Resonators, the dies for the Half Spoke and End Wall are fairly large and complex. Several trials on copper material were tried for fine tuning the die / punch sets to get the required dimensional accuracy as well as to minimize variation in wall thickness, especially at corners and along the e-beam welding edge.

Figure 5 shows the die and punch for the End Wall and Half Spoke. Figure 6 shows the trial pieces of the Half Spoke that has also been machined, End Wall and the Spoke to Shell Collar, all formed in copper. The Spoke to Shell Collar die can also be seen in the picture.
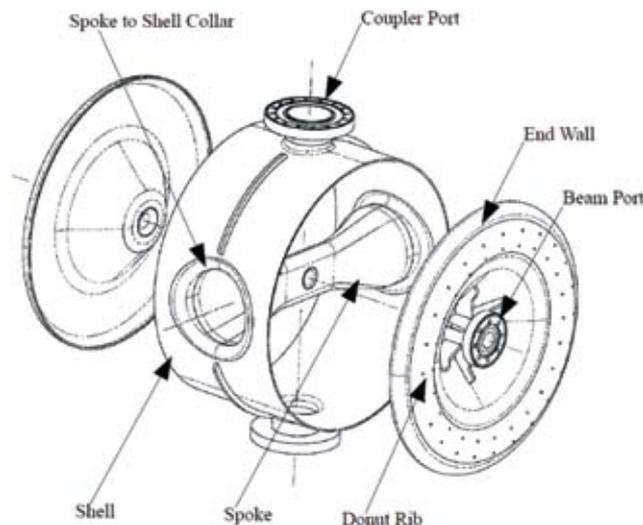
Fig. 4. Single Spoke Resonator (the diameter is approximately 500 mm)

Fig. 5. Dies for forming the End Wall (above) and the Half Spoke (below).

**Fig. 6. Half Spoke (left), End Wall (center) and Spoke to Shell Collar (right)
formed in copper. The forming die for the Spoke to Shell Collar can also
be seen in the foreground of the picture on the right.**

2.1.2.4 Tesla-type Single Cell Cavity

As part of a joint collaborative project, IUAC and Raja Ramanna Centre for Advanced Technology (RRCAT), Indore are developing a Tesla-type Single Cell Niobium Cavity. This project has been taken up by RRCAT to initiate some activity in SRF area for a larger program that is being planned for future. Figure 7 shows the Single Cell Cavity which is approximately 400 mm long. The cavity is made out of high RRR grade niobium except the end flanges which are made out of Nb-Ti alloy.
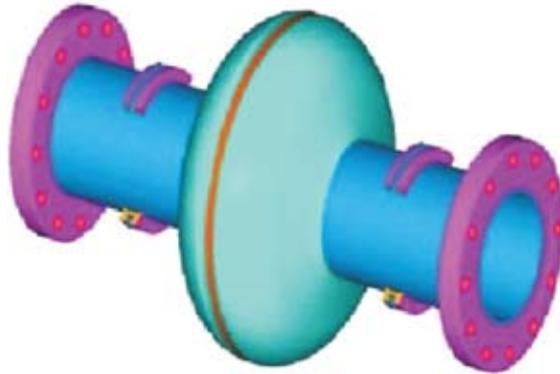
Fig. 7. Tesla-type Single Cell Cavity (the overall length is about 400 mm)

All the dies, machining fixtures, electropolishing fixtures, niobium machining and forming are done at RRCAT. IUAC is sharing its experience in niobium cavity fabrication and several of the fixtures have been designed in consultation with IUAC. Besides this, IUAC is also extending its facilities, namely electron beam welding, electropolishing, heat treatment and mechanical workshop (wherever required) for the fabrication. The first Half Cell of the Single Cell Cavity has been completed (figure 8). Work on the other half cell has also started.

Fig. 8. Niobium Half Cell of the Tesla-type Single Cell Cavity.

2.1.2.5 Repairing of Linac-1 QWRs

The QWRs in the first linac module had been developing vacuum leaks through the welded bellows on the Coupling Ports and they were being replaced by the indigenously developed formed bellows assembly on the Long Coupling Ports (LCP), whereas the Short Coupling Ports (SCP) were being blanked off. The replacement / blanking off work was being done as and when the resonators developed leak. This strategy, however, proved to be ineffective, cumbersome and time consuming. Besides it was hampering the pace of the resonator production and other niobium resonator work. Therefore it was decided to repair all the resonators in the first linac module by replacing the old welded bellows on the LCPs with formed bellows and blanking off the SCPs irrespective of whether they were leaking or not. In all, on 8 QWRs 13 LCPs and 6 SCPs were replaced / blanked off. After the repair work all the QWRs were lightly electropolished before mounting in the cryostat. This has resulted in the cryostat vacuum improving from the earlier value of low 10^{-7} mbar to high 10^{-9} mbar, and even after isolating the turbo molecular pump from the cryostat the pressure did not deteriorate, but infact it kept improving slowly.

The Slow Tuner Bellows used with the QWRs were also repaired by e-beam welding the joint that attaches the upper convolution with the lower one. The welding was performed from the inside, which was infact a very delicate operation. On a couple of Slow Tuners the bellows had come off over 90% of the joint length but they were successfully restored. The Slow Tuners were also lightly electropolished before mounting on the resonators.

2.2   CRYOGENICS

T.S.Datta, J.Chacko, A .Choudhury, J. Antony, M. Kumar, S. Babu,   Soumen Kar, R.N.Dutt,P. Konduru, A. Agnihotri, R.G. Sharma and A.Roy

In this academic year, a single cold test has been performed for offline testing of resonators in the beam line cryostats of rf-Superconducting LINAC. Performance of off-line tests is reported in Linac section.

2.2.1   Cryogenic Facility

I.   *Liquid Helium Plant*

The helium plant was operated five times, out of which one run was in close loop mode for off-line testing of all the eleven resonators of buncher cryostat, 1st Linac module and rebuncher cryostat and four runs for off line testing of resonators in simple test cryostat. The approximate running time was 300hrs and estimated total production of LHe was ~ 30000 l which is significantly lower than the last year due to single close loop run for Linac. Most

of the time in this academic year, the resonators which were leaking had gone through the systematic repairing work.
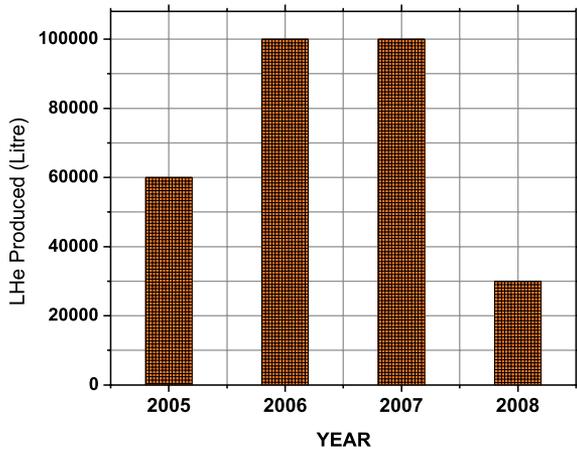
Fig. 1. Yearly Liquid Helium production
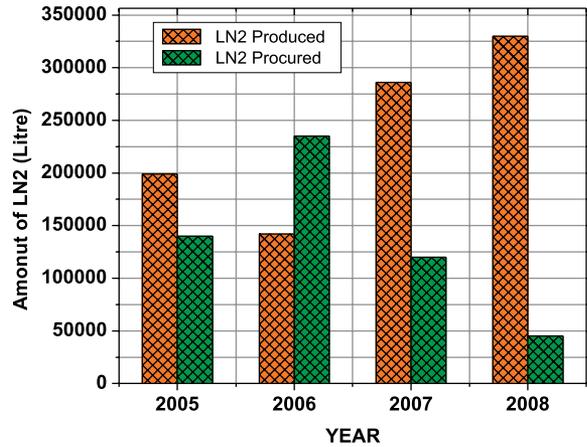
Fig. 2. Yearly Liquid Nitrogen production

Poor performance of Cold Expansion engine w.r.t higher cool down time and lower refrigeration capacity forced us to open the engine without any support from the Principal. Problems were identified and rectified and performance with respect to production rate improved than earlier but still less than specified capacity. A systemic performance test has been planned in refrigeration mode rather than liquefaction mode. Refrigeration mode does not demand higher engine speed as compared to liquefaction mode and lower speed may be one of the reasons to have poor performance. Since the demand was lower, the plant was operated at lower speed and with optimum pressure (200 psig) to have minimum wear and tear of engine and compressor. Operation of helium refrigerator through 2 x 300 KVA UPS helped us to run Linac with minimum human interference and with minimum helium loss.

II.   *Liquid Nitrogen Plant*

The plant was operated for 6000Hrs and estimated liquid nitrogen production was 3, 30,000 L which is significantly higher than last two year which is shown in fig. [2]. LN2 procured from outside vendor was considerably reduced to 45,000 L.   The LN2 distribution line coming from outer LN2 storage tanks   was removed during the construction of the HCI building and a flexible line was installed temporarily. . It was difficult to fill the liquid in INGA LN2 Dewar (~ 1000L) from outer LN2 tanks using the flexible distribution line due the higher heat in leaks in this flexible line. During major Linac runs in this period demand of LN2 were managed by only internal supply. The operation frequency of the plant was increased and the production rate was also enhanced from 50- 75 litres to 100- 150 liters/hr. by upgrading PSA capacity and modifying return flow cycle.

III.   *Liquid nitrogen Distribution Line*

Vacuum jacketed Liquid Nitrogen transfer line (~ length of 125 mts) with on line isolation valves and vacuum break to connect external storage vessel to existing network with an extension to INGA LN2 storage vessel was planned, designed with detailed component specification. Fabrication and supply order for this line was placed with M/S INOX India Ltd . Choosing Bayonet connection in place of welding between different pool sections minimized site work. A vacuum jacketed venting line for liquid nitrogen has also been planned all along the beam line cryostat to connect different nitrogen vapour venting points of all cryostats using bayonet joints.

Performance Report of Cryostats

I.   *1st LINAC Module*

There was a single off-line test of all the resonators in the 1st Linac module.   Resonator could achieve the highest accelerating field so far in this off-line test. As the leaks in different resonators had been repaired, cryostat could maintain 1.5E-8mbar vacuum at 4.2K without any active pumping by 1500LPS turbo molecular pump. Figure 3 shows the vacuum profile during the cold test.
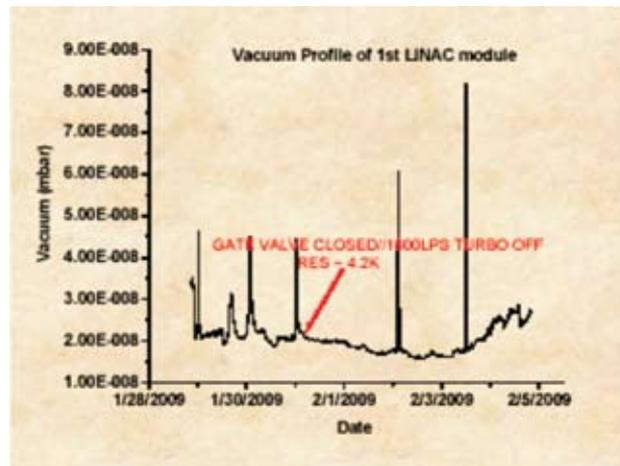
Fig. 3. Vacuum Profile of 1st Linac module

II.   *2nd and 3rd Linac Module*

The fabrication of different components like vacuum jackets, thermal shield, LHe vessels and LN2 vessels of 2nd and 3rd Linac module has been completed in this academic year. At present all the individual components are going through the vacuum leak testing and thermal cycling. The integration of different components with the top plate is under progress.

Some significant modification has been implemented for these two module based on the operational experience of 1st module. To achieve the faster cooldown of resonators, LHe will directly be delivered to the bottom of the resonator through a small LHe manifold inside the LHe vessel instead of top LHe filling in the existing module. Figure 4 and 5 show the vacuum jackets of both 2nd and 3rd Linac module and one of its top plates.

Fig. 4. Vacuum Jackets of 2nd and 3rd Linac Module

Fig. 5. Top Plate of the new Linac Module

Other Development Projects

I. *Development of Cryogen free superconducting magnet system (CFM) with room temperature bore [DST Project]*

I.a *Experimental Test Rig*

Cryogen free superconducting magnet system will not have any active cooling medium like LHe or LN2, therefore makes its own complicacy in design of the system. We had lot of unknown parameters for designing this kind of conduction cooled system within limited refrigeration budget at 4K. A two stage (35W@45K and 1.5W@4.2K) GM cryocooler (CCR) based experimental test set up has been developed to investigate different technical concepts and to generate the design parameters. Figure 6 shows the different components of the test cryostat.

I.b *Experimental simulation on cool-down of magnet equivalent mass*

To simulate magnet cool-down, a copper block weighing 14.5Kg was thermally attached to the 2nd stage of the CCR and it takes 7.5hrs to bring down the temperature of

the dummy mass to 2.75K from room temperature. The minimum temperature achieved on Copper shield with radiation load is 27.45K in 5Hrs. The vacuum achieved is 8E-9mbar at 2.75K. Figure 7 shows the cool down profile of the cold mass and thermal shield.
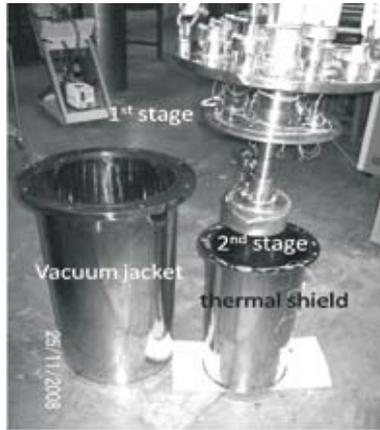
Fig .6.   Inside view of   two stage GM cryocooler integrated test set up
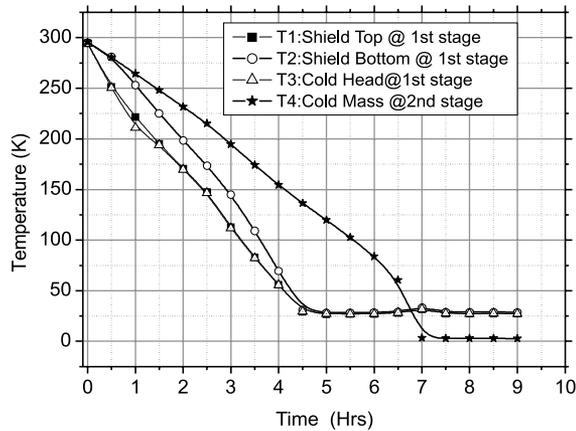
Fig. 7. Cool down profile of magnet equivalent cold mass and thermal shield.

I.c   Current simulation test

The current simulation test has been carried out to study the performance of the hybrid current leads consist of a pair of un-optimized copper leads from 300K to the 1st stage and HTS current leads from 1st stage to the NbTi wire at the 2nd stage. An indigenously developed SMPS power supply (100A and 10V) has been used in current simulation test. The stabilized temperature and corresponding dynamic heat loads have been measured for each operating current. The total heat load (static +dynamic) at 70A turns out to be 18.8W @35.2K for 1st stage. and ~135mW for 2nd stage (2.9 K). Figure 8 shows static heat load, the variation of dynamic heat load and temperature   for the 1st stage of CCR with different circulation current.
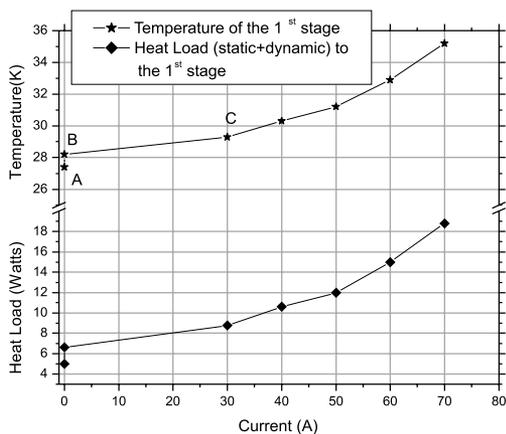
Fig. 8. Heat load (static + dynamic) and temperature of 1st stage   with current
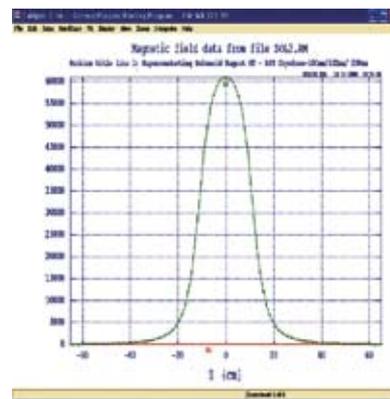
Fig. 9. Axial field profile of 6Tesla S.C. Magnet (Superfish)

I.d   Performance of electrical isolation and thermal anchoring of HTS leads

The joints between room temperature currents leads and HTS current leads have been thermally anchored and electrically isolated from the thermal shield cooled by the 1st stage of CCR and similar technique has also been followed for the joint at the 2nd stage between HTS leads and NbTi wire. We have evaluated aluminum nitride (5mm disk) and Kapton tape (60µm thick) as the two alternatives for thermally conducting and electrical isolated joints at both the stages.

I.e   Design of the 6Tesla Magnet

We have optimized the design parameters of the magnet (inner and outer winding diameters, winding length and field uniformity) using 0.54mm NbTi wire for 6T central field with 0.08% uniformity in 10mm DSV at 90A.

Fig10. Winding Machine developed at IUAC

We have also analyzed the axial field profile of the   magnet and field mapping in the cryostat using SUPERFISH program.   Figure 9 shows the axial field profile of the magnet.

I.f   Development of Winding machine

A versatile winding machine has been developed to wind the solenoid magnet made of round wire and the pancake magnet made of flat HTS tape. The machine has the capability of winding HTS tape along with a 60µ kapton as insulation. Figure 10 shows the newly developed winding machine.

II.   HYRA Quadrapole Cryostat

A superconducting quadrapole cryostat has been planned at IUAC for its nuclear research programme in the HYbrid Recoil Mass Analyzer (HYRA) beam line. The cryostat

consists of quadrupole doublet structure with super-ferric iron cover and will be used to focus the nuclear reaction products with large solid angle of acceptance. The estimated cold mass at 4.2K is 1.8 Ton and is mainly contributed by iron core and pole along with coil. Considering the space restriction on the existing cryo-line and operational problems on refilling of LHe, it is planned to have a cryostat fitted with a cryocooler. Based on estimated heat load and commercial availability a two stage cryocooler of capacity of 1.5watt@4.2K at 2nd stage and 35watt@45K at 1st stage is proposed. In this configuration 2nd stage will re-liquefy liquid helium evaporated from the helium vessel. The first stage of the cryocooler will provide the cooling necessary to maintain the intermediate shield to ~50K to reduce the head load on the second stage of cryocooler. It is proposed to use 2 pairs of HTS current leads to supply ~100A of current to NbTi coils for getting the required 2.2T magnetic field. Design optimization of the cryostat is done based on the available refrigeration capacity of the cryocooler and so a detailed heat load input map from various input sources to the cryostat has been studied both theoretically and experimentally and is restricted to well with in the capacity of the cryocooler. Another important feature of the cryostat will be to put flexibility in design so that the helium vessel inside can be positioned in three dimensions to align it with the beam axis when in cold condition. The estimated heat load for the 1st stage is 35.5 W and the corresponding temperature will be 45K. Similarly it will be 800mW and 4.1K for the 2nd stage. Figures 11 and 12 show the schematic view of the cryostat and it's inside view. The fabrication order has been placed to M/S Vacuum Techniques, Bengaluru.
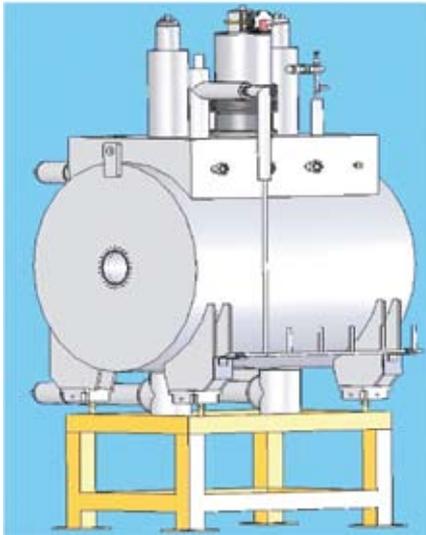
Fig. 11. Final view of Quadrupole Cryostat
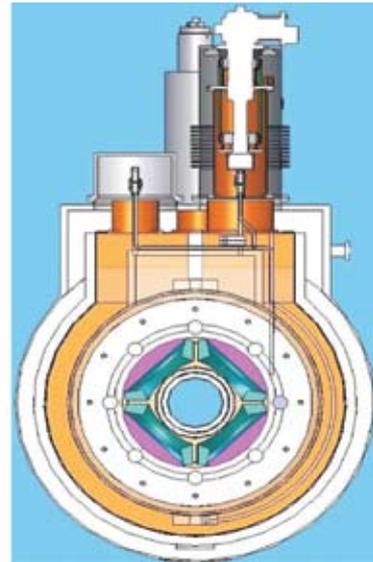
Fig. 12. Inside view of Cryostat

III. *Helium Gas separation by using membrane [BRNS Project]*

A (BRNS) project has been undertaken to see the feasibility of helium gas separation from nitrogen or air by the use of cellulose acetate membrane module. The motivation for

the project of helium separation from nitrogen gas was to see if helium gas can be purified at room temperature without the use of cryogenic adsorber at LN2 temperature. India has a vast resource of thorium and found in the costal sand as monazite sand. In processing of the same it was earlier found in another study that the concentration of helium gas coming out of it is ~ of 20%-30% and rest is nitrogen mostly.

Although separation of helium and nitrogen is well established by the use of cryogenic technique but handling the same at field level is rather difficult since it requires a lot of infrastructure, supply of cryogen from distant source, and trained manpower. Separation of nitrogen gas from oxygen by the use of membrane is a very well established technique. Recently hydrogen gas separation from other gas constituents is being actively pursued by this technique. The usefulness of this technique is that it requires minimum infrastructure and also minimum human intervention as far as the process is concerned and all the process takes place at room temperature
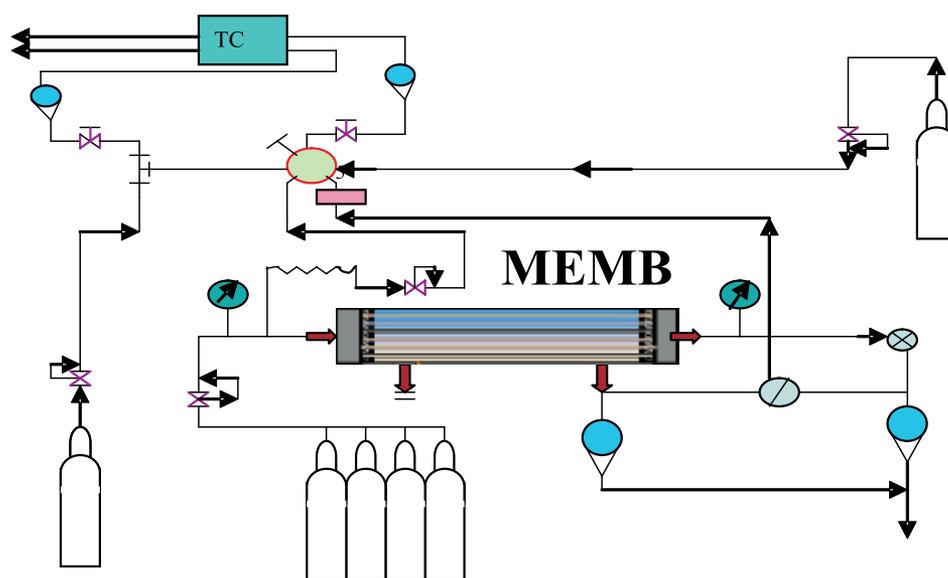
Fig.13. Schematic of the Membrane based Helium Gas purification set up

We planned to investigate the feasibility of separation of helium gas from nitrogen gas through the use of membrane in this project. As a part of this project we have been able to procure a membrane from M/s Airliquide. A set up, which is shown in figure 13, has been made to study the various membrane parameters which include a gas manifold capable of making various combinations of gases, membrane module, a TCD GowMac analyzer and flow meters. The analyzer module has been calibrated with 20 number of calibrated gases the set up has just been commissioned and preliminary result is very encouraging. We are trying to get a few other membrane modules from other manufacturers and see their performance.

IV.   *Development of High Temperature superconducting (HTS) Pancake Magnet*

Soumen Kar, Rajesh Kumar, G. Rodrigues

The indigenous development cryogen free 1.8T solenoid magnet using stainless steel laminated Bi-2223 tape has been initiated for 18GHz ECR ion source. Magnet will consist of five pairs of double pancake coil with nine numbers of HTS to HTS joining. In-situ joining of these high strength SS laminated tapes on the former is more complicated because of their temperature limitation during soldering and it's SS lamination gives higher joint resistance. The ends of the SS laminated tape of each pancake could be extended with silver clad HTS tape using overlap joint and bridge joining could be used for silver clad HTS tape to join two pancake coils. We have studied both types of joining procedure and the joint resistance has been calculated from the I-V characteristics of overlap joint between SS laminated HTS tape and silver clad HTS tape with different overlapping lengths and the corresponding critical current ratio (CCR) has also been measured following the $1\mu V/cm$ criterion at 77K. Typical joint resistance achieved is $0.08~\mu\Omega$ with 15cm of overlapping and its corresponding CCR is 80%. The joint resistance has also been measured for the bridge joint between two silver clad tapes with different no of bridges. The joint resistance achieved with six bridges is $0.1\mu\Omega$ at 77K. All the above results have been compared with the measured joint resistance of bridge joint between two SS laminated HTS tapes. Winding of the magnet would be done once the reproducibility of joint development is achieved.

2.3   RF ELECTRONICS

A. Sarkar, S. Venkataramanan, B.K. Sahu, A. Pandey & B.P. Ajith kumar

2.3.1   Status Report of the Multi-harmonic Buncher & the High Energy Sweeper and associated jobs

The multi-harmonic buncher (MHB) was operated along with the low energy chopper (LEC) to provide 4 MHz pulsed beams to 3 different users. In the first run, ^{19}F beam pulses with FWHM ~ 1 ns was delivered. During the second run, ^{32}S with FWHM ~ 1.2ns was delivered. The third run used ^{16}O beam with 1ns FWHM.

During the Linac Run of December'07, it was observed that the centroid of the beam pulse shifted with any change in the Pelletron parameters and it was quite difficult at times to get the centroid back to the old position. This made the Linac operation quite difficult. In order to understand the root cause of the problem three stability runs (May'08, Oct'08 & Nov'08) were taken in which MHB alone, MHB + LEC and MHB + HES(high energy sweeper) were operated. The parameters affecting the centroid shift were studied.

A thorough off-beam test was conducted and the stability of the phase locking electronics for MHB was studied. Few changes were made in the phase locking circuitry to improve the stability of the centroid. After these changes a beam test run was conducted which showed quite improved stability of the centroid. A circuitry for correcting the HES phase using the HES slit currents was also studied during this run.

2.3.2 Development of a piezoelectric based control scheme for superconducting resonators

Though resonators are working fine with present fast and slow tuner based control scheme, investigations are going on for more reliable operation of the resonators using a piezoelectric actuator to control the amplitude and phase of the accelerating fields. The piezoelectric tuner working in ~ milli seconds range with the dynamic phase control scheme will share a substantial load from the electronic tuner. Also it will help us an alternative to the existing mechanical tuning using high purity helium gas, which is complicated and expensive. A study and development of a piezoelectric tuning mechanism with our existing fast tuning control scheme based on Dynamic Phase Control method for the phase locking of the resonator was tested.

The Piezoelectric crystal of Physik Instrumente (PI) make was connected to the bottom of the niobium mechanical tuner of the resonator. It was powered by a supply in the range of -19 to 100 V to measure its total tuning range. The frequency variation with the Piezoelectric tuner attached with a QWR was measured to be ~2.5 kHz and ~626 Hz at room temperature and at 4.2° K respectively. To keep the superconducting cavity phase locked during operation with dynamic phase control, the piezoelectric voltage should vary with phase error to compensate the drift during phase locked condition of the cavity. To achieve this, a PI based control scheme is planned. The aim of this control scheme is to compensate the frequency drift around central frequency of the cavity and eliminate the hysteresis effects. PI based control scheme was built to compensate the frequency drift around the central frequency of the resonator and to eliminate the hysteresis effects by generating an appropriate voltage for the piezoelectric tuner according to the phase error of the resonator controller. During the cold test first we phase locked the superconducting resonator with resonator controller after making the frequency equal to master frequency by adjusting the P-I control reference value in the summing amplifier. Then the phase error signal from resonator control is reduced to 10 times by a gain block of .1 and given to the input of P-I control unit. The output of the P-I control unit is given to the modulation input of the high voltage piezoelectric Amplifier. We observed that the slow drift in the resonator central frequency is compensated by varying the piezoelectric actuator voltage. When drift is fast and of large amplitude the resonant goes out of lock but again captured by piezoelectric actuator within sec. The overall average power requirement for control is almost within 10 % of the quiescent power. The stability of the lock was observed with accelerating field E_a=2.2 MV/m at 100Watt of forward power. The amplitude and phase lock stabilities were measured to be 0.1% and 0.4 degree respectively

at this field level. At higher field we observed the amplitude instability in the resonator and since the Drive coupler movement was not very smooth and it had enough backlash we could not set up a higher field for locking with required frequency bandwidth. For a short duration we were able to lock at accelerating field more than 3 MV/m but the average power was more than 200 Watt and the cavity went out of lock after a while. We have successfully demonstrated the piezoelectric actuator based control scheme for superconducting quarter wave resonators. The dynamics of this control scheme can be improved to make it more effective for locking the resonators at higher field gradient. Also since the piezoelectric actuator based tuning mechanism gives limited tuning range a coarse tuning approach is planned using a stepper motor in future.

2.4 BEAM TRANSPORT SYSTEM

A.Mandal, Rajesh Kumar, S.K.Suman, Mukesh Kumar and Sarvesh Kumar

Beam Transport System laboratory takes care of regular maintenance, design and development of Accelerator beam Transport System. This year the detail beam optics for Low Energy Ion Beam facility has been worked out. Beam optics for HCI is being simulated for various options. Different beam transport elements viz quadrupole magnets, electrostatic quadrupoles, beam diagnostic elements etc are being developed for LEIBF and HCI. Power supplies for different magnets have been indigenously developed. Other than power supplies the group is actively involved (in collaboration with other groups) in development of equipments like superconducting magnets, instruments for beam modification and material characterisation. Details of development activities are summarized below.

2.4.1 Design of new Low Energy Ion Beam Facility

The new low energy ion beam facility to be installed at Material Science Building has been designed which consists of many features over old facility such as more beam lines, higher deck voltage, large acceptance analyzing magnet and better extraction geometry. The facility consists of an ECR ion source placed on 400KV deck, an Analyzing cum switching magnets having three beam lines for Atomic and material science research. A general lay out of the facility is shown in figure .The beam optics simulation and design of the switching magnet was reported last year. Further beam optics calculations with various beams and charge states have been performed. The various parameters of the optical components have been optimized so as to transfer beams with deck voltage varying from 30 KV to 300 KV. It has been observed that to transport beam of low energy, emittance has to be reduced. TRANSPORT and GIOS code have been used for optical simulations. A typical transverse beam optics for the Argon ion beam simulated for different charge states at a fixed acceleration potential of 300kV including space charge effects are shown in fig. 1a. The layout of components of new LEIBF is as shown in fig. 1b.

34

The design specifications of the switching magnet are given in table 1. The beam optics of switching magnet has been carried out by using simulation program TRANSPORT and GIOS. For a fixed object distance, the image distance for different beam lines after switching magnet decreases with increase in bending angle because the focusing strength of the bending magnet is more for higher bending angles. For 75 deg. beam line the image distance has been optimized along with a quadrupole triplet after switching magnet. For 90 deg. and 105 deg. beam lines, Separate quadrupole triplets have been used to focus beam at target positions downwards.

Table 1 : Specifications of Switching Magnet

Bending Angles (deg.)	75, 90 , 105
Bending Radii (mm)	641.75, 529.1, 460
Pole Gap (mm)	65
B_{max} (T)	1.55 @ 240Amps
Entrance Angle (deg.)	29.05
Exit Angles (deg.)	15.95, 30.66, 43.09
Max. ME/q^2 (MeV. amu)	44.68, 30.37, 22.96
Momentum Resolution (δp/p)	$\approx 3.7 \times 10^{-3}$
Homogeneity (δB/B)	$\leq 10^{-3}$
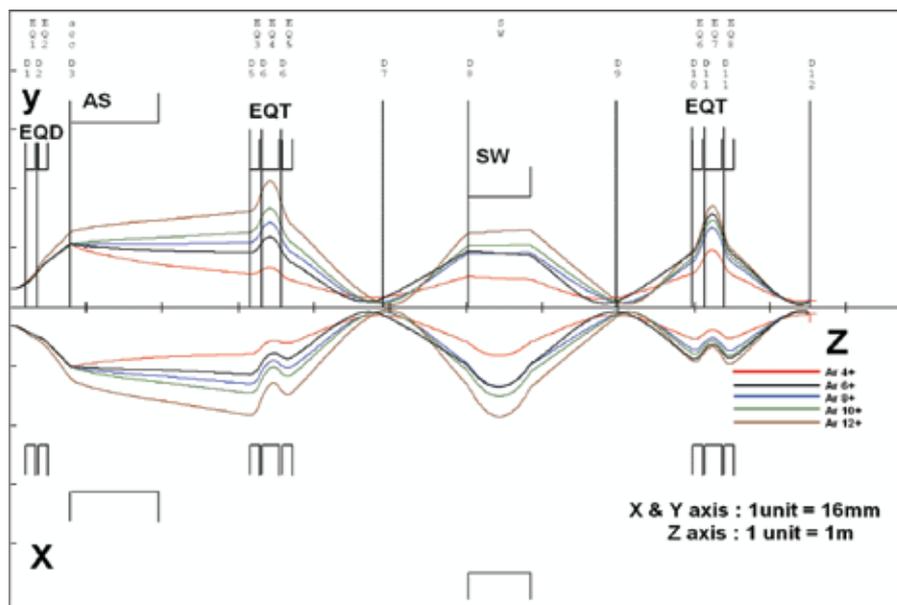
Fig. 1a. Beam Optics of 90^0 beam Line using TRANSPORT code at 10 kV extraction and 300kV acceleration after adjusting beam diagnostics components
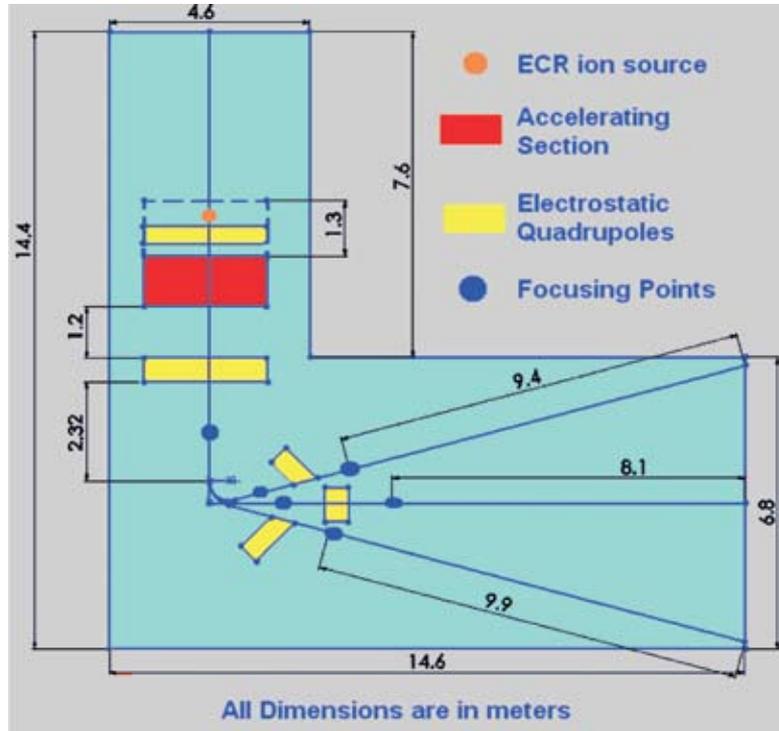
Fig. 1b. Layout of new LEIBF in Mat. Sc. Building

2.4.2 Beam Optics of High Current Injector

The low energy beam transport (LEBT) section of the High Current Injector (HCI) consists of the high temperature superconducting ECR ion source PKDELIS, magnetic quadrupole doublet (MQD), a large acceptance 90° analyzing magnet (AM) with maximum magnetic rigidity of 0.09Tm, an accelerating section (AS) with deck potential of 30kV and a few focusing devices to transport the beam from ECR ion source to the entrance of 48.5 MHz radio frequency quadrupole (RFQ). At the exit of ion source, an emittance of 200 π mm-mrad has been considered which would be transported through the low energy beam transport section to the entrance of RFQ. The ions from the ECR source would be first extracted around 30 kV and then mass analyzed by large acceptance analyzing magnets and further accelerated. These ions of energy 8keV/u are transported to RFQ using quadrupole focusing elements and would be then matched to initial beam parameters of RFQ. The codes TRANSPORT, GIOS and TRACE 3D have been used for simulation of beam dynamics. The transverse beam optics for LEBT section is as shown in fig. 2a. The layout of high voltage deck is given in fig. 2b.

As RFQ and DTL are designed to accept comparatively less emittance coming from superconducting ECR ion source and thus we have to limit the emittance after the analyzing magnet to 80 π mm-mrad by a double slit so as to pass through the successive components. A multi harmonic buncher of fundamental frequency 12.125 MHz will be placed at the waist of the beam formed after the accelerating section. It will bunch the incoming dc beam to a few

36

ns and then the bunched beam is matched to initial beam parameters of RFQ section using a set of four magnetic quadrupoles
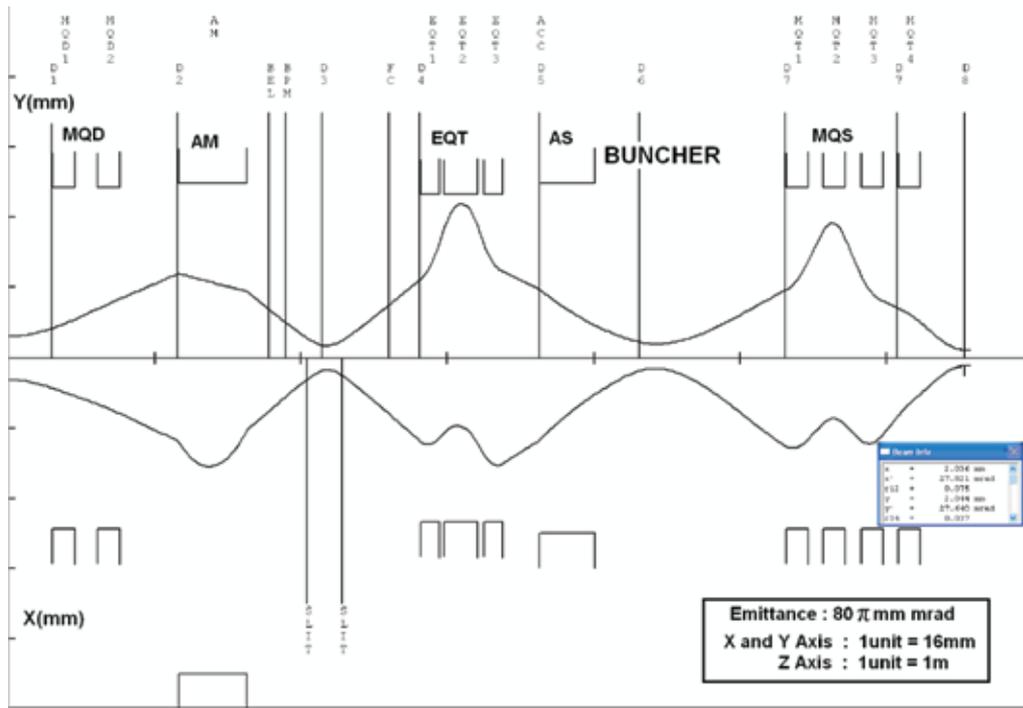
Fig. 2a. Transverse beam optics of LEBT section of HCI using TRANSPORT code
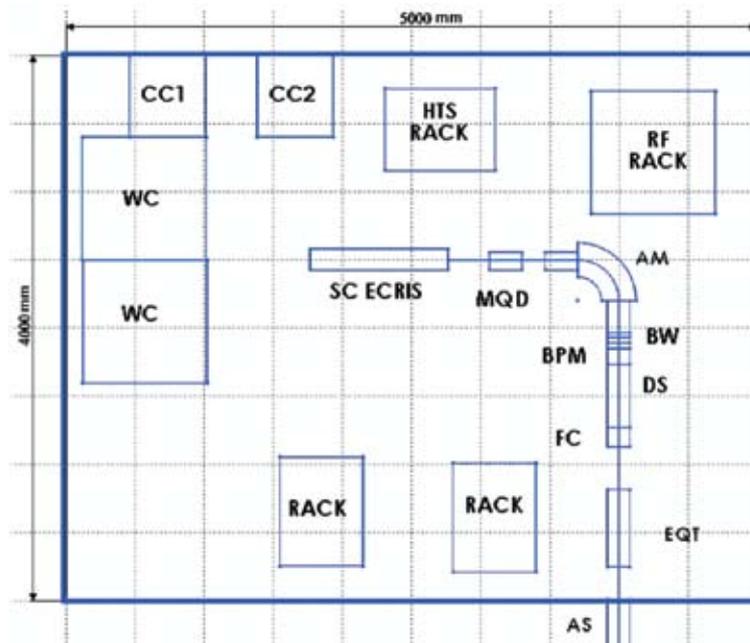
Fig. 2b. Layout of high voltage deck of high current injector

2.4.3 Measurement of the uniformity of the irradiated material due to scanning by Scanner magnet

Srashti Gupta, A.Mandal, D.K.Avasthi, Amit kumar Chawla

Accelerator delivers the ion beam of spot size 2mm on the sample of size 2cmx2cm. Most of the irradiation experiments in material science need large area of the sample to be exposed by ion beam. Therefore to perform uniform irradiation over large area, a good quality scanner is required. The electromagnetic scanner is widely used in accelerator facility for homogeneous irradiation of sample over a large area by ion beam. The magnetic scanner developed at IUAC, Delhi is being used routinely in material science beam line for irradiation of samples of size 2cm*2cm. Uniformity of irradiation is important because of proper characterization of irradiated material. We have developed a method to measure the uniformity of irradiation. The method involves measurement of the tracks created on a quartz sample irradiated by an energetic beam, using SEM. The details of the experiment and the results are presented here.

A quartz sample (1cmx1cm) was irradiated by Ni^{+8} beam of 110 MeV Energy delivered by pelletron at IUAC. The fluence was $10^9 ions/cm^2$, current 0.15 pnA, time of irradiation was 2 sec.

Irradiated samples were etched in 48% aqueous HF solution for different timings (30 sec, 1 min, 2min, and 5 min) at room temperature. After Etching all the samples were washed immediately in deionized water.

Surface of the etched sample were investigated by the Field Emission Scanning Electron Microscopy (FE-SEM) at IIT Roorkee. Pore density in different region of a sample (Quartz) was counted using by SEM.

Pore density as measured in different regions of quartz sample (1cmx1cm) is shown in table 2. The image of the tracks in different regions as seen through FE-SEM is shown in fig. 3. from which it is clear that numbers of pores in different regions of quartz are approximately same. The mean value of the no. of pores is calculated $\sim 215 \pm 18$, where 18 is the standard deviation (σ) value. The data shows that variation of the no. of pores in different region of sample lie within 2 σ value. This implies that the uniformity of irradiation of sample is within 95% confidence level.

Table 2 : Comparison of tracks in different region of sample

Sample	Area	No. of pores
Quartz A	5x5μm (4different places at corner of sample)	228,254,198,232
Quartz A	5*5μm (5different places at the center of sample)	218,198,210,199,206
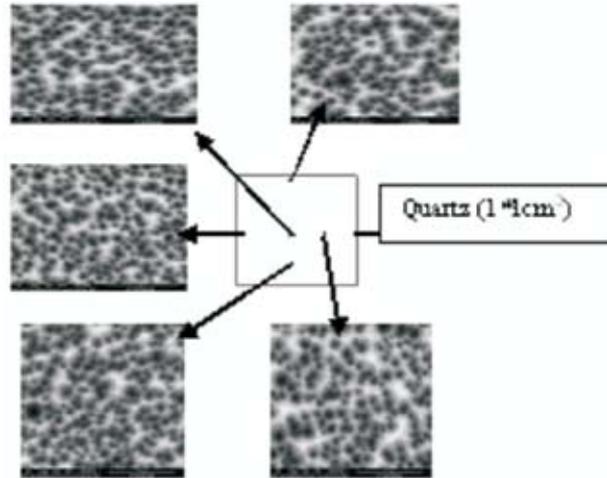
Fig. 3. SEM image of etched ion tracks in different region of etched quartz irradiated with Ni beam with energy 110 MeV, fluence 1.8*109 ions/cm², etching time 30 sec

2.4.4 HYRA quadrupole power supplies

Rajesh Kumar, S.K. Suman and Mukesh Kumar

Fabrication of four numbers of high current high stability power supplies have been completed last year for HYRA quadrupoles with following specifications:

300A, 32V	: 2nos.
330A, 42V	: 2nos.
Stability (8hrs.)	: 10PPM

These power supplies have been installed and connected to magnets and tested with magnets for local as well as remote (CAMAC) control setup. The short term stability test (8hrs) of each power supply has been carried out and found to be less then 10 ppm at full output rating with actual load. These power supplies are being used in test runs and experiments carried out at HYRA. No performance degradation (drifts) and operational malfunctioning was reported by the user during this period.

Fig. 4. HYRA quadrupole power supplies

2.4.5 High current scanner magnet power supply fabrication

S.K. Suman and Rajesh Kumar

High power scanning magnets are used in Ph-II beamline. The power supplies for these are high current true bipolar current regulated transconductance linear amplifiers specially designed to power inductive loads. The amplifier has been provided with CAMAC interface for remote operation. Four such amplifiers have been fabricated and tested. The power supply has the following specifications & features:

Output current range : 0 – 100App for X and 0 – 160App for Y-scanning
Output voltage range : 0 – 100Vpp for X and 0 – 20Vpp   for Y-scanning
Scanning frequency range : 0 – 50 Hz   for X and 0 – 10 Hz   for Y -scanning
True current regulated triangular wave output without crossover distortion.
Over voltage & Over current protection.
Remote / local operation.
Necessary safety interlocks.
Status indication on front panel as well as for CAMAC (remote) read.

Fig. 5. High current scanner magnet power supplies

2.4.6   Quad. & Steerer magnet power supply development for HCI facility

S.K. Suman, Rajesh Kumar and Mukesh Kumar

In HCI beam line different types (low current, high current, unipolar, bipolar) power supplies will be used. To minimise spares inventory for different power supplies, we have designed and developed common regulation and control electronics which can be used to control all types of required power supplies. This also will help for easy, fast maintenance as well as manpower training. Design has been completed and one prototype for each type of following has been tested.

7V, 25A unipolar power supply for quadrupole
12V,5A   unipolar power supply for quadrupole
±50V, 5A bipolar power supply for steerers

It is current regulated linear power supply. It has necessary safety interlock, status display and can be operated locally or remotely (CAMAC). It consists some common electronics like interlock card, front panel interface, IGOR interface and front panel electronics similar to HYRA power supply. The following new modules have been developed particularly for HCI power supply.

Universal Regulation module for unipolar/ bipolar operation
Transistor bank Interface for unipolar/ bipolar operation
Forced air cooled transistor banks for unipolar/ bipolar operation

Fig. 6. HCI magnet power supply

2.4.7   CAMAC based dual channel controller for scanning magnet power supply

S.K. Suman and Rajesh Kumar

A single width CAMAC based controller has been developed for remote operation of high current scanning magnet power supply. Necessary controls and functions have been provided to operate both X&Y power supplies on a single module. The controller provides isolated triangle wave in response to 0-10V signal. The frequency of the triangular wave is set at 50Hz for X-scanning and 0.2 Hz for Y-scanning which can be changed by changing internal jumper. It also provides ON/OFF commands and 8-bit readback register. An additional DC offset features has been incorporated for steering the beam.

Fig. 7. CAMAC based controller for scanning magnet power supply

2.4.8 16 bit Input gate output register fabrication

S.K. Suman, Rajesh Kumar and Mukesh Kumar

All DC current regulated magnet power supplies in the beam transport system are controlled remotely through CAMAC based IGOR module. It provides 16-bit Input gate and 16-bit output register with handshaking, two control pulses and one status bit. All input/output signals are HTL type for controlling the power supplies at a distance of about 15 meters from CAMAC crates. 40 such indigenously developed modules are already used in Ph-I& II. This year fifty more modules have been assembled and tested for future HCI facility.

Fig. 8. 16 bit Input gate output register

2.4.9 Super conducting magnet power supply and Programmer fabrication

Rajesh Kumar and S.K. Suman

15 numbers of power supplies and power supply programmers (designed in 2001-02) have been assembled/fabricated and tested for different types of supper conducting magnets presently under developing at IUAC. The power supply is a 1kW (10V/100A) online PWM based switching supply with current and voltage regulation. Programmer controls the power supply by comparing the magnet current with the desired current function and then producing the appropriate voltage across the magnet which is necessary to achieve the desired current function.

Fig. 9. Super conducting magnet power supply and Programmer

2.4.10 Controlled temperature pulse generator

S.K. Suman and Rajesh Kumar

A controlled temperature pulses generator with a fast slew rate has been designed and assembled to develop a pyroelectric emitter for neutron source system. As both the heating and cooling are required, so a thermoelectric cooler (TEC) based instrument developed with the following specification:

Temp. pulse rising rate (heating) : 2°C/Sec.
Temp. pulse falling rate (cooling) : 0.75°C/Sec.
Pulse Span: 50°C (10°C to 60°C)
Repetition rate: 90 Sec/Cycle

The instrument consists of a thermally insulating box for housing sample holder, temperature sensors for feedback and readback and the TEC device. The TEC fits in between aluminium sample holder and base plate. The base plate is a large heat sink acting as a thermal reservoir. Since the thermal time constant of the base plate is much longer than the sample holder that is why heating and cooling rates are different. The temperature is controlled by a proportional feedback loop so that a constant rate is achieved. A temperature sensor glued at sample holder sends temperature information which is compared with a reference (control ramp signal) for generating an error signal. This error signal is then amplified and sent to the TEC. The TEC then changes the temperature, completing the loop. Since the initial and final values of temperature are not as important as the "rate of change", the ramping range has been taken near room temperature to achieve the largest dynamic range with fast thermal response.

Fig. 10A. Temperature pulse generator
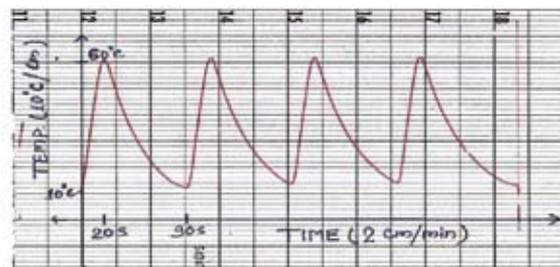
Fig. 10B. Output waveform

2.4.11 Development of tube based 2kW RF amplifier

Rajesh Kumar, Rajkumar and C.P. Safvan

The initial aim of the development is to understand the working of loop control, metering and biasing power supply requirements of tube based RF amplifiers. This will help in future development and more important in maintenance of tube based RF

amplifiers (high power) which will form an integral part of the upcoming accelerator facility.

Fig. 11. Tube based 2kW RF amplifier

The biasing power supplies (Plate & Filament), output power control loop and metering circuits including safety interlocks were developed for a 2kW RF amplifier unit. The tube assembly was taken from an existing old RF amplifier unit. All the subassemblies were developed and integrated in a 19" rack to make a standalone amplifier system. The unit has been tested with a resistive load at full output power.

2.4.12 Fast high voltage switch for beam pulsing at LEIBF facility

Rajesh Kumar, Rajkumar and C.P. Safvan

As the low energy ion beam facility provides beams at very low energies, pulsing by conventional multiharmonic buncher is not feasible due to long travel distances required. Therefore a chopper type of beam pulsing system has been developed for the LEIBF. A fast high voltage pulse applied to a pair of sweeper plate perpendicular to the beam direction in combination with a slit would provide a small beam bunch.

Fig. 12. Fast high voltage switch

For this purpose a High speed High Power MOSFET with very low parasitic inductance has been used. To achieve the fastest rise time (1ns) a low inductance/ capacitance circuit/ assembly has been developed with following precautions-low inductance components, short and low inductance connections, dynamically current carrying lines as short as possible and star type grounding. Optimised snubbers have been used to damp oscillations due to parasitic inductance which are dominant due to high di/dt. The switch has been assembled, installed at LEIBF and achieved 2nS turn-on rise time at 3kV.

2.4.13 High voltage(±2kV) bipolar amplifier to power electrostatic scanner/ sweeper

Rajesh Kumar, Mukesh Kumar and S.K. Suman

A high voltage, linear bipolar amplifier with three channels (for X1-axis, Y1-axis and Y2-dog leg plates) has been designed for use in scanning and steering applications of ion beams. The unit has been provided with both local and remote controls. In response to ±10V control signal at the input the unit delivers ±2kV at the output. The unit can be used to operate electrostatic steerers (the three channels can be used for dog-leg operations) or can be used as beam sweepers to sweep the beam across target samples at high frequencies to attain uniform irradiation/implantation. The instrument has been designed in a 19" card frame assembly. All the sub assemblies are card frame type modules interconnected and powered through backplane PCB.

2.4.14 SCR based single phase power controller

S.K. Suman and Rajesh Kumar

A SCR based single phase power controller has been developed. It can be used as a pre-regulator in linear power supply to control the power dissipation across series pass device (transistor bank) to replace the vario transformer, so that physical size and cost of power supply may be reduced. The pre-regulation is essential in case of air cooled power supplies to minimize power dissipation.
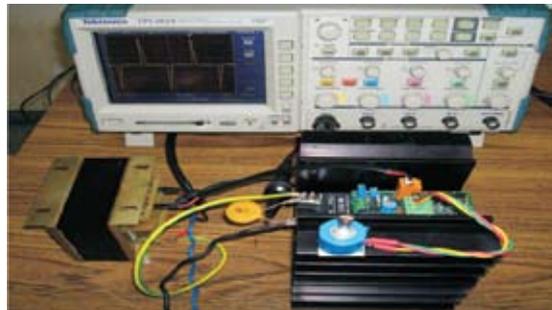
Fig. 13. SCR based single phase power controller

2.5   LOW ENERGY ION BEAM FACILITY   (LEIBF)

P. Kumar, D. K. Mishra, G. Rodrigues, P. S. Lakshmy, U. K. Rao, Y. Mathur and D. Kanjilal

The performance of LEIBF [1,2] has been satisfactory in academic year 2008-2009. Various beams were extracted from the ion source and delivered successfully for experiments related to materials science, atomic and molecular physics. The facility, LEIBF, is unique in the sense that it can deliver ion beams in the energy range of a few tens of keV to a few MeV. This energy range is most suitable for investigating many research problems in various fields of science, especially in materials science. Gaseous beams were developed using direct gas feed method. However, for the development of Ni beam, metal ions using volatile compounds (MIVOC) [3] method was used. The platform voltage was kept below 150 kV to avoid the sparking problem during the operation of ion source. Experiments on beam transmission from analyzer magnet to experimental chambers were done. We also studied the uniformity of ion implantation with the help of beam scanner. For this experiment, we used polymer samples over which area of implantation was clearly visible due to color contrast. A technical report on the detail of this experiment was submitted to academic cell. The beam profile of BPM installed in post analyzer section was marked for best ion beam transmission and focusing conditions. For implantation/irradiation, we have a high vacuum chamber with special sample holders for mounting large numbers of samples. We have provision for heating the samples at a maximum temperature of 500^0C using PID temperature controller. Implantation at LN_2 temperature is also possible.

We had minimum maintenance work during last academic year due to regular check of electronic and mechanical components installed in beam line and ion source. Major maintenance works during last year were the repairing of gas dosimetry valve controller, 200 W traveling wave tube (TWT) amplifier, and dry vacuum pump installed on HV platform. We also replaced turbo molecular pump installed in experimental chamber. The old pump had completed recommended hrs of operation and was making   much noise while running at full speed.

Improvement of one order of magnitude in vacuum of experimental was noticed after the replacement of old pump. The source, beam line and experimental chamber pressures are low 10^{-7}, high 10^{-8} and low 10^{-7}, mbar respectively.

Apart from production and delivery of ion beams for user experiments, we preformed an experiment where we have Ni ions for the synthesis of ZnO based dilute magnetic semiconductor.100 keV Ni ions were implanted in ZnO single crystal using LEIBF. The fluence was varied from 4.9×10^{15} to 1.1×10^{16} ions/cm^2, which corresponds to the variation of dopant concentration from 3% to 7%. No remarkable change was observed in the optical band gap of implanted samples. The atomic force microscopic studies showed formation of nano rod like structure having average length of 240 nm in 5% Ni implanted ZnO (shown in Figure 1). There was no appreciable change in basic crystal structure and no Ni precipitate was observed. The magnetic hysteresis obtained for 7% Ni implanted ZnO showed the room temperature

ferromagnetism (shown in Figure 2). One of the reasons of appearance of room temperature ferromagnetism in 7 % Ni implanted ZnO seems to be due to the defects produced by ion beam implantation and may be called as ion beam implantation induced room temperature ferromagnetism. Implantation of Ni in ZnO and subsequent annealing are expected to lead to synthesis of controlled diluted magnetic semiconductor (DMS) structure in ZnO.

The light ions (H and He) implantation was mainly done for defects engineering of materials, specially semiconductors like Si, AlN, GaN and InP in collaboration with IIT Delhi group. The objective of this work is mainly to optimize the ion fluence for the formation of nano/microcracks in implanted semiconductors. Further, implantation parameters (ion current, ion energy, processing temperature) were optimized to get the controlled blistering in these semiconductors. The preliminary results on these studies are encouraging and presented in related conferences.
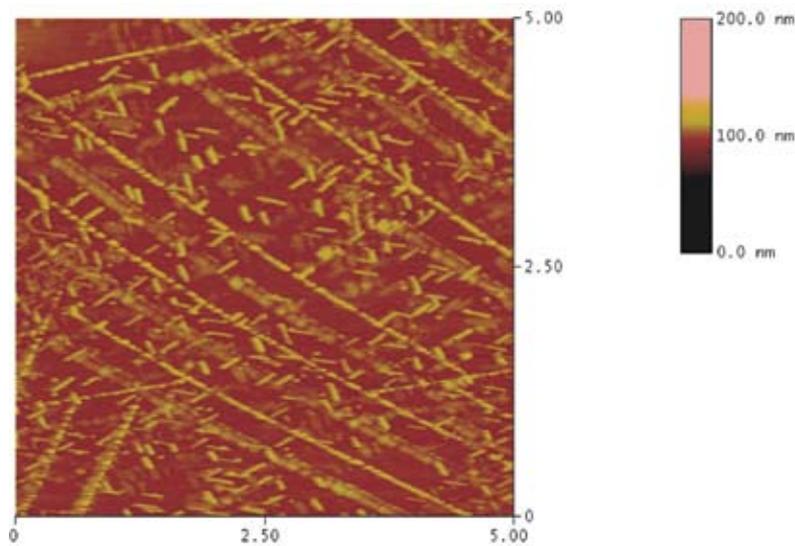
Fig. 1. AFM picture of 5% Ni implanted ZnO
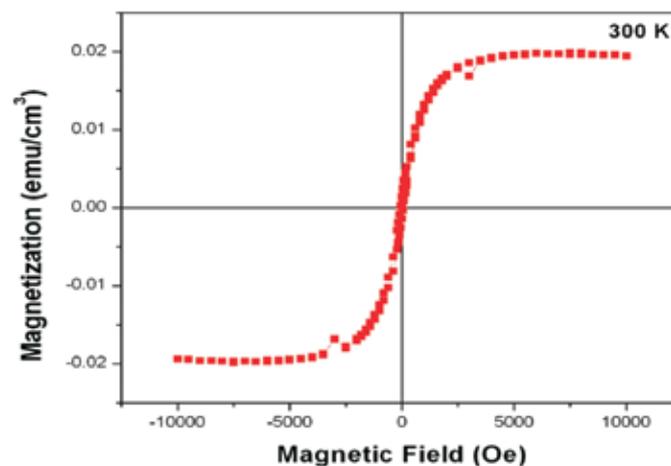
Fig. 2. Magnetic hysteresis curve of 7 % Ni implanted ZnO.

We are also in process of shifting the LEIBF in new building. For this, a double storey high voltage (400 kV) platform was designed and installed in the beam hall (LEIB building). A new DANFYSIK switching magnet with three exit ports has also been positioned. The high voltage testing (400 kV at 0.5 mA) of deck was completed. The ion optical design of new LEIBF was done using various simulation codes and finalized in position and dimension of various beam line components.

The LEIBF has been operational almost full time for delivery of various ion beams for experiments related to materials science, atomic and molecular physics. The typical experiments, which were carried out, include synthesis of nano structures and dilute magnetic semiconductors (DMS), ion beam re-crystallization, phase formation, structural changes in polymers, ion beam mixing, fundamental ion-matter interactions, molecular dissociation by ion beams etc. Such experiments resulted in large number of publications in international referred journals. More than one dozen Ph.D students completed their Ph.D using this facility. A two days workshop (9-10 July 2009) is further planed to discuss possible internationally competitive experiments using LEIBF. The best poster presentation award of Indian Particle Conference (InPAC) 2009, second best oral presentation award of COCHIN NANO-2009 (second international workshop on frontiers in nano science and technology), best poster presentation award of DAE-DRNS symposium on atomic, molecular and optical physics 2009 was given to the work associated with LEIBF.

REFERENCES:

[1]   D. Kanjilal, T. Madhu, G. Rodrigues, U.K. Rao, C.P. Safvan, A. Roy, Indian J. Pure Appl. Phys. 25 (2001) 39.

[2]   P. Kumar, G. Rogrigues, D. Kanjilal, A. Roy, Beer Pal Singh, R. Kumar, Nucl. Instr. and Meth. B, 246 (2006) 440

[3]   P. Kumar, G. Rogrigues, P. S. Lakshmy, D. Kanjilal, Beer Pal Singh, R. Kumar, Nucl. Instr. And Meth. B, 252 (2006) 354

2.6   HIGH CURRENT INJECTOR

The high current injector is being developed as an alternate source of ion beams into the superconducting LINAC. The various parts of the high current injector namely the PKDELIS ion source, the radio frequency quadrupole accelerator and the drift tube linac accelerator are in various stages of development and are described below:

2.6.1   High Temperature Superconducting ECRIS -PKDELIS and Low Energy Beam Transport System (LEBT)

G.Rodrigues, P. S. Lakshmy, U.K.Rao, Y.Mathur, R.N.Dutt, P.Kumar, A.Mandal and D.Kanjilal

A.   Source Operations

During the last year, the source vacuum has been improved mainly at the injection side and this has resulted in improved beam currents for the medium and highly charged ions. The turbo pump at the injection region was found to be going bad possibly due to the axial magnetic field and this was rectified by re-positioning the pump and with additional µmetal shielding. The two gas injection lines (using Teflon tube) were also found to be leaking from the gas panel and this was rectified and positioned on the source body using all-metal sealing. Typical base pressures at the injection side and post analyser section   are 3×10^{-7} mbar and 1×10^{-8} mbar. A typical spectrum optimised on Ar^{8+} at an absorbed power of 300 W is shown in figure 1. The optimised parameters were RF power, gas pressure, bias voltage, axial field and position of the RF tuner. These were the main determining parameters besides the extraction voltage (for improving the transmission) for obtaining 300 µA of Ar^{8+} (fig 1.) at 300 W absorbed power   without using mixing gases.
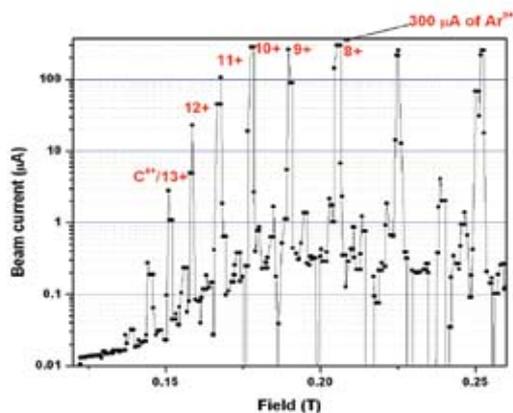
| Fig. 1. CSD optimized on Ar^{8+} | Fig. 2. CSD optimized on Ar^{11+} |
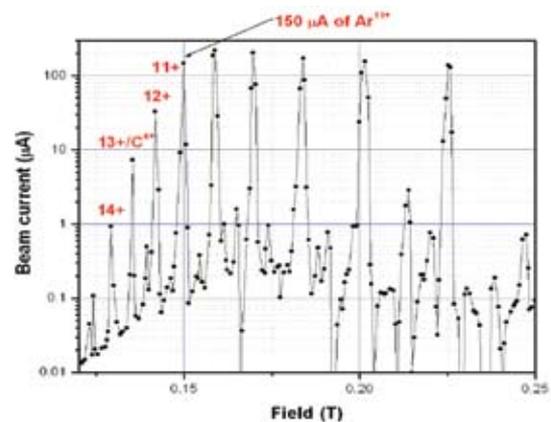
Use of mixing gas with argon, the beam current of Ar^{8+} is expected to improve further. Due to a leak in the mixing gas line, it was not possible to further improve the beam currents at present. Further optimisation on Ar^{11+} at higher levels of power showed that it was possible to extract 150 µA of Ar^{11+} (Fig 2.) at 425 W of totally absorbed power. During the tuning and optimisation of Ar^{8+} and Ar^{11+} beams, it was observed that the best axial field distribution corresponds to B_{min}/B_{ecr} of 0.58 which is calculated from the observed injection and extraction fields. This value does not change for medium (8+) and high charge state (11+) of argon although the value of the extraction field changes slightly. Further improvements in the gas injection line/pumping system are being pursued.

B. Source diagnostics

Besides the beam optimisation experiments of argon for medium and high charge state, it was necesssary to measure the x-ray Bremsstrahlung and if possible to correlate with

the beam optimisation experiments for argon. Alternatively, these measurements could give further information on the source performance. Therefore, it was decided to measure the x-ray Bremsstrahlung using NaI detector due to the higher efficiency as compared to a germanium detector. X-ray Bremsstrahlung was measured using a 3 inch NaI detector from the ECR plasma along the extraction side through the 0° port of the analysing magnet. A schematic of the set-up to measure the x-ray Bremsstrahlung is shown in figure 3. Special care was taken to shield the detector using Pb bricks and to collimate the x-ray Bremsstrahlung from the plasma only. Besides the plasma electrode having an aperture of 6 mm, three additional collimators are used for proper collimation as shown in the figure. One collimator of diameter 2 mm, length ~ 50 mm and made of aluminium was positioned on the analysing magnet 0° exit port at a distance of 1645 mm from the plasma electrode. An additional collimator made of lead and having a diameter of 5 mm and length 2 mm (positioned at a distance of 1380 mm from the first collimator) was sandwiched on to another collimator of diameter 8 mm and length 50 mm. The detector was positioned behind the last collimator with proper lead shielding around it using 50 mm thick lead bricks. Due to the high count rate, the distance between the detector and the source had to be increased. The x-ray spectra were measured as a function of negative bias voltage keeping the extraction voltage OFF with each measurement taken for 900 seconds (shown in figure 4).
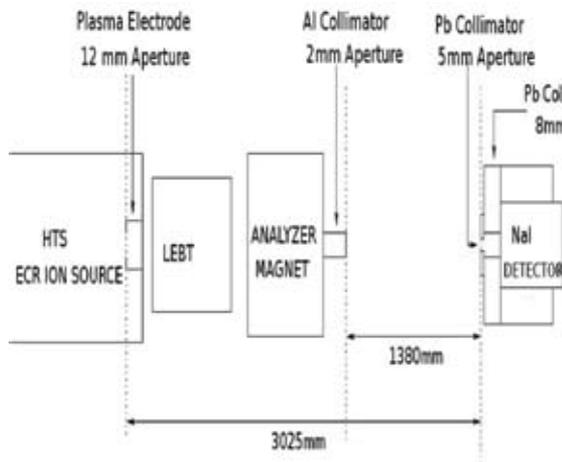
Fig. 3. X-ray Bremsstrahlung set-up   Fig. 4. X-rayBremsstrahlung spectra
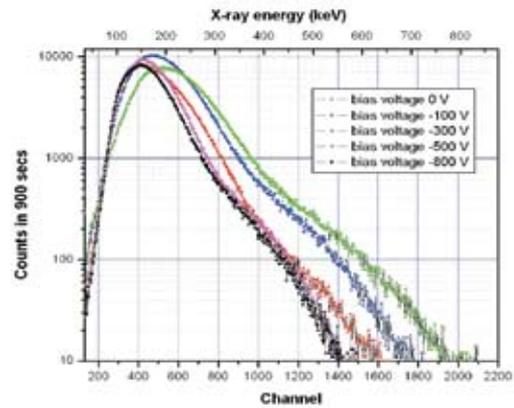
C. Optics for the low energy beam transport

The optics from the source upto the post-analysed faraday cup has been looked into some detail (see earlier annual reports for schematic of the LEBT). Extraction voltages around 15 kV to 20 kV have been found to be optimum for reasonable transmission and also for stable operation. However, higher extraction voltages beyond 20 kV causes over-focussing and the transmission through the system deteriorates. A beam viewer (quartz) just before the post-analyser faraday cup clearly shows that the beam is focussed (y-direction) at a position somewhere up-stream of the quartz which also roughly matches with the simulations Further modifications are going on to improve the transmission through the LEBT.

50

D. Two-frequency operation studies

As a part of the improvement of the source performance, adding an additional frequency (two-frequency operation) has added benefits as observed from various ECR sources around the world. In order to explore the possibility, we have tried to simulate the ECR surfaces for various frequencies corresponding to operating magnetic fields. Frequencies lower than 18 GHz are always possible due to the magnetic field structure; however, higher frequencies are limited due to the maximum operating magnetic fields of 1.8 and 1.5 tesla for the injection and extraction sides respectively. The simulation shows the optimised ECR surfaces which correspond to typical operating currents of 120 A and 80 A on the injection and extraction coils for highly charged ions like Ar^{11+} etc. The minimum frequency that can allow us to operate is roughly 12.6 GHz corresponding to Becr of 0.45 T. Figure 5 shows a cross-sectional view of the ECR surface in the horizontal plane with corresponding resonance fields.

Source testing with TWT amplifier
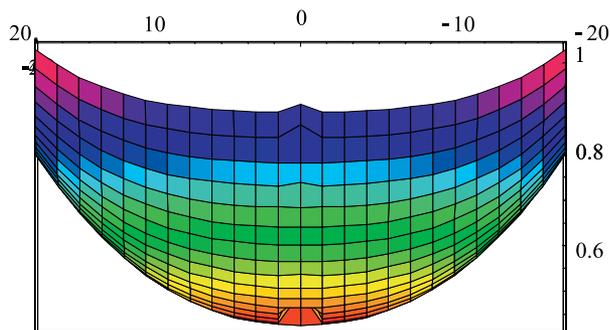
Fig.5. Cross-sectional view of ECR surfaces
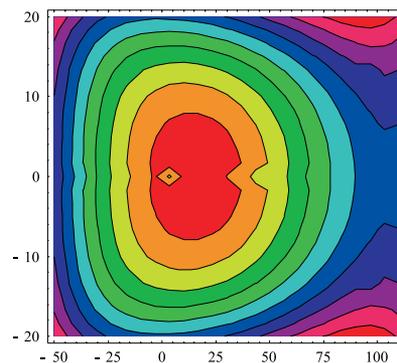
Fig.6. Contours of ECR surfaces
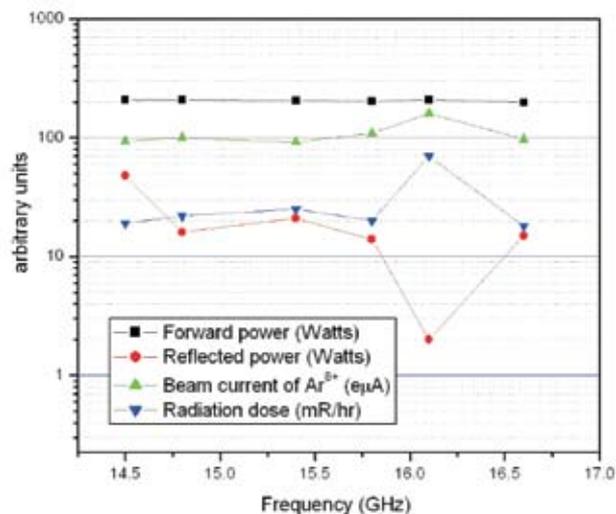
Fig. 7. Measured parameters as a function of input frequency.

51

It is being planned to operate the source with two discreet frequencies to further improve the ionisation efficiencies and extracted beam currents. Incorporating an alternate klystron poses constraints on the space available. Alternatively, it is clearly seen that the performance of the TWT's are much better when compared to klystrons and occupy much lesser space but at reduced power levels. In order to obtain some preliminary data on the microwave power coupling into the plasma chamber for frequencies ranging from 14.5 up to 18.0 GHz (second feeding frequency), a 200 W Travelling Wave Tube (TWT) amplifier was utilised for this purpose. A 1-20 GHz Rohde & Schwarz signal generator was used to set the frequency keeping the input power level fixed at –4 dB. At each input frequency, the source was optimised for the best possible current of Ar^{8+} and keeping the forward power and gas pressure constant. Figure 7 shows the dependence of the Ar^{8+} beam current, reflected power and x-ray radiation dose level as a function of the input frequency. Due to losses in the cables at frequencies higher than 16.6 Ghz, further measurements could not be taken up to 18.0 Ghz. The minimum reflected power at 16.1 GHz shows maximum power coupling into the plasma chamber at that frequency. Better power coupling attributes to an increased electron density which results in an increased beam current and x-ray radiation dose as seen in figure 7. Development of an additional microwave injection line for the second frequency is underway.

E.   Design of magnet structure for a 2.45GHz ECR Ion Source

As a part of ion source development programme, a permanent magnet 2.45GHz ECR ion source has been planned to develop indigenously at IUAC. A permanent magnet structure for the 2.45GHz ECR ion source which is capable of producing high intensity low charge state ion beams is designed and part of the fabrication process is in progress. NdFeB magnets are used and arranged in the form of two coaxial rings having 6 segments in each ring, around the plasma chamber. A stainless steel, magnet pole holder has been designed for assembling the magnet segments in such a way that each pole can be locked separately after mounting the magnet segment inside the pole holder. Fig. 8 shows the schematic view of the pole holder with the side plates and the pole clamps which are used to lock each magnet slot after mounting the magnet piece.

The plasma chamber is being designed using a double walled, water cooled cylinder of 100mm in diameter and 180mm in length The permanent magnet produces a field of 0.12 T at the center of the chamber. An iron yoke has been put in between the magnet rings for clamping the field at the center of the plasma chamber. A trim coil at the center of the magnet assembly provides fine tuning of the axial magnetic field distribution near the resonance field (875G). Permanent magnet rings have been made movable, which adds flexibility in tuning the magnetic field distribution. A schematic view of the magnet assembly and the axial magnetic field distribution are given in Fig (9) and Fig (10) respectively. In Fig (10), legend A shows the field distribution obtained with the magnet-iron yoke assembly while legend B and C show the corrections achieved with the trim coil. Figure 11 shows the 2.45 GHz, 2 kW rf injection line and associated quarter wave transformer.
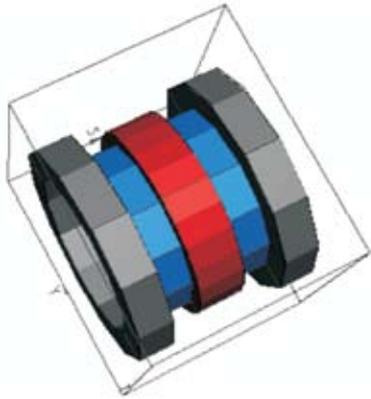
Fig. 9. A schematic view of the magnet structure
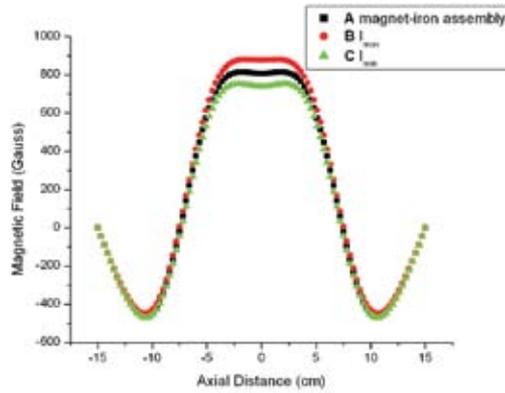
Fig. 10. Axial magnetic field distribution

Fig. 11. View of the 2.45 GHz, 2 kW RF injection line (left) and quarter wave transformer (right)

REFERENCES

[1] C. Bieth, S. Kantas , P. Sortais , D. Kanjilal , G. Rodrigues , S. Milward, S. Harrison , R. Mc Mahon, Nucl.Instrum.Meth., B 235 (2005)498

[2] D.Kanjilal, G.Rodrigues, P.Kumar, A.Mandal, A.Roy, C.Bieth, S.Kantas, P.Sortais, Review of Scientific Instruments,77,03A317 (2006)

[3] A. Mandal,, G. Rodrigues, D. Kanjilal, Peter Brodt, Franz Bødker, Nuclear Instruments and Methods in Physics Research A 583 (2007) 219–227

[4] R.Baskaran, T.S.Selvakumaran, G.Rodrigues, D.Kanjilal, A.Roy, Review of Scientific Instruments,79, 2008

[5] A.Mandal, G.Rodrigues, D.Kanjilal, A.Roy, Physics Procedia 1 (2008)105, Proceedings of the Seventh International Conference on Charged Particle Optics

2.6.2 Low Power RF Tests On The 1.17m Modulated Prototype RFQ Accelerator

C.P. Safvan, Sugam Kumar, R. Ahuja, A. Kothari, R.V. Hariwal, D. Kanjilal

The proposed 48.5 MHz Radio Frequency Quadrupole (RFQ) was designed to accelerate ions with A/q of 7 from 8 keV/A to 180 keV/A. Looking at the limited space available and beam dynamics consideration the A/q has been changed from 7 to 6. This has reduced the RFQ length from 4m to around 2.5m with external buncher. The DTL length has been also reduced considerably. The ion beams produced by the ECR (PKDELIS) source will be injected into the RFQ and be further accelerated to just above 2MeV/A by a drift tube Linac (DTL) working at room temperatures, velocity matched beam with □= 0.08 will be injected into superconducting LINAC, which will further accelerate the ions to 5MeV/A. Earlier initial unmodulated 1.17 m prototype of the 48.5 MHz RFQ is designed, constructed, installed and studied to determine the final specifications for modulated RFQ accelerator.

The modulated vanes have been fabricated at IGTR Indore and successfully installed for low power RF tests. The cavity is equipped with various ports where the input inductive loop for power coupling and output loop for probe is installed.

The system is able to achieve high vacuum level (10^{-7} torr) with the help of single turbomolecular pump. The RFQ vanes and vane supports were being fabricated at Indo-German Tool Room Indore and Ahmedabad. The whole electrode assembly is inserted in RFQ cavity.

A convex bend of around 3mm height was found on the lower plate of cavity while assembling the modulated vanes. With the help of DonBosco this was machined and corrected within the error limit. The alignment of the modulated vanes is done successfully within around 150 micron level accuracy. Water channels are being made which is essential to dissipate heat and stabilize the resonance frequency during high power RF test.

Automated bead pull system has been set up for the measurement of cavity parameters like resonant frequency, Quality factor, Shunt impedance, Power required, Electric field mapping and Quadrupole symmetry. Programs are written using LabView Software. For accurate bead positioning and its position measurement an automated light detective instrument is also setup. Bead pull accessories like high dielectric ruby bead, nylon thread, rf components etc. is acquired to perform rf test. Self Exciting Loop (SEL) electronics being optimized to excite the cavity at designed frequency.

The RF parameters measured are listed below. The resonance frequency and intrinsic quality factor measured are 53.02MHz and 2355 respectively, while ideal (simulated) values are 48.5MHz and 4000. Shunt impedance is found to be 23.66 k-ohm as compare to 80 k-ohm, which is, designed value of unmodulated part. Power required to generate 70kV Intervane voltage is coming out to be 43.21kW, while with 30kW of input power, which is also designed input power; 57.8kV of Intervane voltage can be achieved.

The major difference found is shift in the resonance frequency at higher value to ideal frequency after modulation. Metallic plates have been placed between upper ridge of rod and

upper plate of the cavity to bring down the frequency at desired value. But due to large shift in frequency of more than 12% and practical limitation to place metallic plate at symmetric position the quadrupole symmetry is lost. Now we are trying to place the plate on inner flange at beam entrance making capacitance with vanes end without disturbing the rod symmetry, this will preserve the quadrupole symmetry.

Low power RF tests being done without rf sealing and surface treatment. Measured intrinsic quality factor value is lower than designed value. This is subject to discontinuity like joints at high current region and high material resistivity of stainless steel comprising base plate and cavity wall.

Although the RFQ rods and its supports are made of copper, the outer chamber and the base plate are made of Stainless steel (SS304) which provides high a resistance path to the current and causes a low quality factor. To improve the quality factor we are electroplating the inner surface of the cavity and base plate with copper for 50-100 micron thickness.

Presently we are working on the electroplating of the chamber. Tuner and its electronics yet have to be designed. The 35kW RF amplifier is getting developed at IPR Ahmedabad. Its each component has been tested separately. We have to work for the designing of the RF power coupler before the beam test. In the next year high power RF and actual beam tests are planned.

Fig.1. Copper electroplating of side plate of RFQ chamber

2.6.3 Status report on the fabrication and testing of the prototype IUAC DTL-IH tank

B. P. Ajith Kumar, J Zacharias, R Mehta, R.V.Hariwal and C. P. Safvan

The High Current Injector project at Inter University Accelerator Centre uses a Radio Frequency Quadrupole (RFQ) and Drift Tube Linac (DTL) combination to accelerate heavy

ions, A/q ≤ 6, from an ECR ion source to inject them to the existing superconducting LINAC. The DTL has been designed to accelerate ions from 180 keV/u to 1.8 MeV/u, using six IH type RF resonators operating at 97 MHz. The required output energy of the DTL is decided by the minimum input velocity of nearly 6% of velocity of light (i.e.β = 0.06) required for the existing superconducting LINAC. IH type resonators are the preferred choice for multiple gap DTL applications due to their high shunt impedance values. The frequency of operation is chosen as 97 MHz after comparing with the 48.5 MHz option. The later offers a larger acceptance but the size of the resonator becomes much larger at this frequency. The beam dynamics and generation of the drift tube geometry is done using the LANA code. The electrical design of the first resonator tank has been done using CST Microwave Studio. Frequency and electric field profile measurements have been done on a full size prototype resonator.

A) *Low Power RF Tests on Prototype IH DTL*

The cavity was designed in CST Microwave studio. The specified frequency is 97 MHz. The prototype is fabricated using SS304 material. Flanges and all ports are welded in and the vacuum test was carried out successfully. The cavity has an inner diameter of 85 cm and length of 38 cm after final fabrication. The ridges which hold the stems of the drift tubes are made from aluminium, and the stems and drift tubes are made from copper as well as aluminium. The 11 gap IH structure has 10 drift tubes, each supported alternately from top and bottom. The machining of the ridges, stems and drift tubes has been done using the in house CNC vertical milling machine. Provision for water cooling has been made in each of the stems as well as the end walls of the cavity. The final cavity will be copper plated so that the power dissipation is within acceptable limits. Low power RF tests were conducted on the prototype cavity. Figure 1 shows the prototype during assembly.

Fig. 1. Photograph of the prototype cavity

For determining the various parameters, bead pull tests and network analyzer based measurements were carried out. The measured resonant frequency of the prototype was near 98 MHz and it was brought to the design value of 97 MHz by using a tuner plate on one side. A bead pull test was done to measure the electric field profile. A sapphire bead was pulled along the beam axis of the cavity and the resonant frequency measured. The shift of the resonant frequency caused by the presence of the bead is proportional to the electric field at the position of the bead. The figure 2 shows the electric field profile along the beam axis. It can be seen that even though the uniformity of the electric fields in the central gaps has been achieved to a large extent, the end gaps have a smaller field than expected. This discrepancy can be explained by the end gaps that were larger than specified due to manufacturing issues, and will be corrected in the final tank.
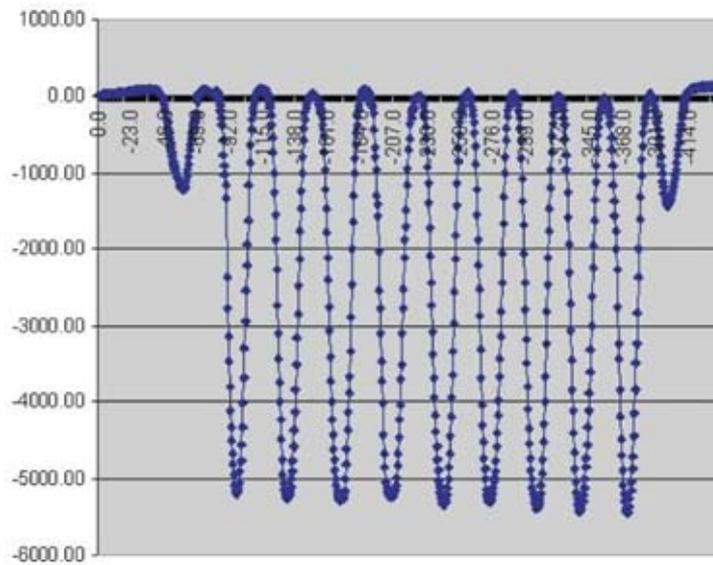
Fig. 2. Bead pull measurement data

B) *Beam Dynamics*

Each IH tank is independently phased from separate rf amplifiers. With the exception of the first and last tank the tanks consist of bunching sections and accelerating sections. The accelerating sections in the IH tanks are designed for 0° synchronous phase. The beam is injected into the accelerating sections with a reduced phase spread and velocity higher than the design velocity so that the bunch drifts to more negative phases during acceleration and emerges with a reduced energy spread. Quadrupole triplets between tanks provide periodic transverse focussing. Short -60° sections at the entrance of every accelerating tank provide periodic longitudinal focusing to allow matching to the next accelerating section. Key to achieving an improved longitudinal acceptance is the addition of an extra long drift-tube between the bunching and accelerating sections to further reduce the phase spread entering the accelerating section. With this novel technique a beam of more than 3π keV/u-nsec can be accelerated with minimal emittance growth. The velocity of the incoming beam ($\beta = 0.02$

) and the chosen resonant frequency (97 MHz) results in a gap length of about 1.5 cm for the first resonator. The inner diameter of the tube is fixed at 1.4 cm to minimize the penetration of field into the tubes. The length of the tanks are chosen in such a way that for the given input emittance (e = .3 π mm mr normalized), the maximum beam size inside any drift tube is less than half of the tube inner radius. A schematic of the proposed DTL along with the transverse beam envelopes are shown in Figure 3. Length and number of cells in each tank along with the output energy after each tank is shown in table 1.
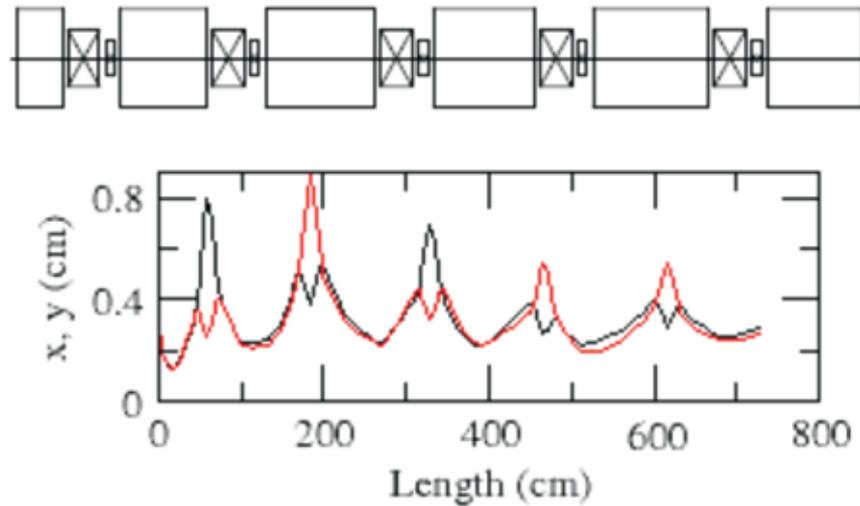
Fig. 3. Schematic of the DTL and the beam envelopes for a normalized input emittance of 0.3 mm mr. The big rectangles represents the cavities and smaller ones represents the diagnostics boxes and magnetic quadrupole triplets.

Table 1: Length, number of cells and output energy for the six cavities.

Length (cm)	Number of Cells	Output Energy (MeV/u)
38.5	11	0.32
73.4	13	0.55
94.4	13	0.85
86.5	11	1.15
92.2	11	1.46
81.6	9	1.8